ORIGINAL ARTICLE

Journal of Cachexia, Sarcopenia and Muscle 2021; **12**: 1098–1116
Published online 11 June 2021 in Wiley Online Library (wileyonlinelibrary.com) **DOI:** 10.1002/jcsm.12740

Survival motor neuron deficiency slows myoblast fusion through reduced myomaker and myomixer expression

Nikki M. McCormack[1], Eric Villalón[2,3], Coralie Viollet[4], Anthony R. Soltis[4,5], Clifton L. Dalgard[1,4,6], Christian L. Lorson[2,3] & Barrington G. Burnett[1]*

[1]*Department of Anatomy, Physiology, and Genetics, Uniformed Services University of the Health Sciences, F. Edward Hébert School of Medicine, Bethesda, MD, USA;* [2]*Bond Life Sciences Center, University of Missouri, Columbia, MO, USA;* [3]*Department of Veterinary Pathobiology, College of Veterinary Medicine, University of Missouri, Columbia, MO, USA;* [4]*Collaborative Health Initiative Research Program, Uniformed Services University of the Heath Sciences, Bethesda, MD, USA;* [5]*Henry M. Jackson Foundation, Bethesda, MD, USA;* [6]*The American Genome Center, Uniformed Services University of the Health Sciences, Bethesda, MD, USA*

Abstract

Background Spinal muscular atrophy is an inherited neurodegenerative disease caused by insufficient levels of the survival motor neuron (SMN) protein. Recently approved treatments aimed at increasing SMN protein levels have dramatically improved patient survival and have altered the disease landscape. While restoring SMN levels slows motor neuron loss, many patients continue to have smaller muscles and do not achieve normal motor milestones. While timing of treatment is important, it remains unclear why SMN restoration is insufficient to fully restore muscle size and function. We and others have shown that SMN-deficient muscle precursor cells fail to efficiently fuse into myotubes. However, the role of SMN in myoblast fusion is not known.

Methods In this study, we show that SMN-deficient myoblasts readily fuse with wild-type myoblasts, demonstrating fusion competency. Conditioned media from wild type differentiating myoblasts do not rescue the fusion deficit of SMN-deficient cells, suggesting that compromised fusion may primarily be a result of altered membrane dynamics at the cell surface. Transcriptome profiling of skeletal muscle from SMN-deficient mice revealed altered expression of cell surface fusion molecules. Finally, using cell and mouse models, we investigate if myoblast fusion can be rescued in SMN-deficient myoblast and improve the muscle pathology in SMA mice.

Results We found reduced expression of the muscle fusion proteins myomaker ($P = 0.0060$) and myomixer ($P = 0.0051$) in the muscle of SMA mice. Suppressing SMN expression in C2C12 myoblast cells reduces expression of myomaker (35% reduction; $P < 0.0001$) and myomixer, also known as myomerger and minion, (30% reduction; $P < 0.0001$) and restoring SMN levels only partially restores myomaker and myomixer expression. Ectopic expression of myomixer improves myofibre number (55% increase; $P = 0.0006$) and motor function (35% decrease in righting time; $P = 0.0089$) in SMA model mice and enhances motor function (82% decrease in righting time; $P < 0.0001$) and extends survival (28% increase; $P < 0.01$) when administered in combination with an antisense oligonucleotide that increases SMN protein levels.

Conclusions Here, we identified reduced expression of muscle fusion proteins as a key factor in the fusion deficits of SMN-deficient myoblasts. This discovery provides a novel target to improve SMA muscle pathology and motor function, which in combination with SMN increasing therapy could enhance clinical outcomes for SMA patients.

Keywords Myoblast; Muscle; Spinal muscular atrophy; Myomaker; Myomixer

Received: 16 June 2020; Revised: 5 May 2021; Accepted: 21 May 2021
**Correspondence to: Barrington G. Burnett, Department of Anatomy, Physiology, and Genetics, Uniformed Services University of the Health Sciences, F. Edward Hebert School of Medicine, Bethesda, MD, USA. Tel: (1) 301-295-3506, Email: barrington.burnett@usuhs.edu*

Introduction

Spinal muscular atrophy (SMA) is one of the leading genetic causes of infant mortality affecting 1 in 10 000 live births annually.[1,2] SMA is caused by insufficient levels of survival motor neuron (SMN) protein.[1] SMN protein is encoded by two genes – *SMN1*, the major producer of full-length SMN protein, and *SMN2*, which primarily produces truncated SMN protein. A C-to-T base pair change in *SMN2* results in the exclusion of exon 7 in the *SMN2* transcript and the production of a less stable, truncated protein referred to as SMNΔ7.[3,4] SMA patients have a homozygous loss or deletion of *SMN1* and retention of at least one copy of *SMN2*. While *SMN2* produces some full-length SMN protein, it is unable to compensate for the loss of *SMN1*.[1]

Spinal muscular atrophy is characterized by the loss of lower motor neurons and muscle atrophy causing patients to have severe muscle weakness.[1] SMN is a ubiquitously expressed protein and has pleiotropic cellular roles.[5,6] How loss of SMN contributes to SMA pathology remains unclear.[7] Although SMA is traditionally considered a motor neuron disease, there is increasing evidence showing intrinsic muscle deficits in SMA including reduced clustering of nicotinic acetylcholine receptors in differentiated myoblasts from SMA patients, reduced quantal content, altered myogenic programing in SMN-deficient myoblasts, and smaller myofibre size in SMNΔ7 mice.[8–17] SMA mice display muscle weakness and SMN-deficient muscle has altered molecular composition prior to denervation.[12,17,18] Additionally, our lab and others previously described reduced fusion of SMN-deficient myoblasts into myotubes,[8,13,19] and muscle-specific reduction of SMN results in muscle fibre defects, neuromuscular junction abnormalities, and compromised motor function.[20] Why SMN deficiency impairs myoblast fusion, and ultimately muscle fibre size and function, remains elusive.

Current treatments for SMA patients are nusinersen/Spinraza®, an antisense oligonucleotide (ASO) that corrects the splicing of the *SMN2* transcript to include exon 7, onasemnogene abeparvovec-xioi/Zolgensma®, an AAV9-based gene replacement therapy, and risdiplam/Evrysdi®, a small molecule that modifies the splicing of *SMN2*.[21–24] These treatments prolong lifespan and the time before patients require permanent ventilation.[25–28] However, many patients still fail to achieve normal motor milestones. In one clinical trial, only 22% of nusinersen-treated type 1 SMA patients gained full head control, and only 1% of patients were able to stand.[25] Therefore, there is a need to identify SMN-independent mechanisms, such as those in skeletal muscle, which can be targeted in combination with current therapies to hopefully improve motor function in SMA.[29] Here, we performed transcriptome analysis of skeletal muscle from wild-type and symptomatic SMA mice and found reduced expression of myomaker, a protein required for myoblast fusion and muscle formation.[30,31] Myomixer expression, a second protein required for myoblast fusion also known as myomerger and minion, was also reduced in SMA mouse skeletal muscle.[31–34] We found that both myomaker and myomixer, as well as MyoD and myogenin expression, are reduced in SMN-deficient myoblasts. Restoring MyoD or myogenin expression increased myomaker and myomixer and partially rescued fusion of SMN-deficient myoblasts. Importantly, AAV9-mediated delivery of myomixer in combination with an antisense oligonucleotide that increases SMN expression improves muscle histopathology, motor function, and lifespan of SMA model mice.

Materials and methods

Cell culture

C2C12 cells (Cat. #CRL-1772, ATCC, Manassas, VA, USA) were maintained in Dulbecco's Modified Eagle Medium (DMEM) (Cat. #11995-065, Thermofisher, Waltham, MA, USA) with 10% fetal bovine serum (Cat. #F2442, Millipore Sigma, Burlington, MA, USA) and 1% penicillin–streptomycin glutamine (Cat. #10378-016, Thermofisher). To initiate differentiation, C2C12 cells were cultured in DMEM supplemented with 2% horse serum (Cat. #26050-070, Thermofisher) and 1% penicillin–streptomycin glutamine.

Generation of survival motor neuron knockdown myoblast line

SMN shRNA (Cat. #MSH030207–2-LVRU6GP, Genecopoeia, Rockville, MD, USA) was packaged into a lentivirus using the Lenti-X Packaging Single Shots Kit (Cat. #631276, Takara Bio Inc., Japan). C2C12 cells were infected with a lentivirus containing SMN shRNA. Puromycin-resistant, GFP-positive clones were selected and expanded. Knockdown of SMN mRNA and protein levels was confirmed by RT-PCR and western blot analyses, respectively.

An antisense oligonucleotide (ASO) (Integrated DNA Technologies, Coralville, IA, USA) was designed to bind and repress the SMN shRNA. Cells were plated and 24 h later transfected with 1 μg of SMN shRNA ASO using Lipofectamine 3000 (Cat. #L3000015, Thermofisher). Cells were collected 48 h after transfection and used for either mRNA or protein expression analysis.

Protein expression analysis

Cell and tissues were lysed in 1% NP-40 (Cat. #28324, Thermofisher), 50 mM Tris–HCl pH 8 (Cat. #15568-025, Thermofisher), 150 mM NaCl, and protease inhibitor cocktail (Cat. #04693-159001, Roche, Indianapolis, IN, USA) on ice for

DOI: 10.1002/jcsm.12740

10 min. The lysates were centrifuged at 4°C for 10 min, and the supernatants collected. Protein concentration was determined using the DC assay (Cat. #5000116, Bio-Rad, Laboratories, Hercules, CA, USA) according to the manufacturer's protocol. Protein lysates were resolved by SDS–PAGE (4–12%) (Cat. #XP04122BOX, Thermofisher) and transferred to PVDF membranes (Cat. #1704272, Bio-Rad). The membranes were blocked in 5% milk (Cat. #1706404, Bio-Rad) and probed with mouse anti-SMN (1:1000; Cat. #610647, clone 8, BD Biosciences, San Diego, CA, USA), mouse anti-β-actin-peroxidase (Cat. #A3854, Millipore Sigma), and goat anti-mouse IgG HRP conjugate (Cat. #BML-A204-0100, Enzo Life Sciences, Farmingdale, NY, USA).

Myoblast fusion assay

Wild-type and SMN-deficient C2C12 cells were plated separately and differentiated for 2 days. Cells were then loaded with either QTracker 585 (Cat. #Q25011MP, Thermofisher) or QTracker 655 (Cat. #Q25021, Thermofisher) according to the manufacturer's instructions. Briefly, 10^6 cells were incubated with QTracker at 37°C and mixed every 15 min for 1 h. Cells were washed twice with differentiation media. Cells were mixed and re-plated on coverslips and differentiated for an additional 5 days. Cells on coverslips were fixed with 4% paraformaldehyde and stained with DAPI (Cat. #4083S, Cell Signalling Technology, Danvers, MA, USA). Five images per condition were quantified for each *n*. Cell mixing images were quantified by dividing the number of double-labelled cells by the total number of cells in the field of view.

Myoblast fusion with conditioned media

Wild-type C2C12 cells were plated on coverslips and then differentiated for 24 h. Conditioned differentiation media from wild-type myoblasts were added to either wild-type or SMN-deficient C2C12 cells. New conditioned differentiation media was added every 24 h for a total of 7 days. Cells were fixed with 4% formaldehyde and immunolabelled with an anti-myosin antibody (1:200; Cat. #MF20, Developmental Studies Hybridoma Bank, Iowa City, IA, USA) and DAPI. Five images per condition were quantified for each *n*. Myoblast fusion was quantified by calculating the fusion index (the number of nuclei in myosin-positive myotubes divided by the total number of nuclei).

Satellite cell isolation

We isolated satellite cells from SMA mice and their wild type littermates using a modified protocol from what we previously described[13] and the Satellite Cell Isolation Kit MACS protocol (Miltenyi Biotec). Briefly, tibialis anterior muscles were isolated from PND10 mice and put into plain DMEM in 6-well plate. The muscles were minced, incubated at 37°C in 2 mL of 0.2% type II collagenase, and displaced for 1 h 30 min into the incubation. Samples were passed through a 40 μm cell strainer into a 50 mL conical tube, and 3 mL of media containing DMEM, 5% L-glutamine, 10% FBS (Life Technologies, Grand Island, NY, USA), 20% fetal bovine serum (Atlanta Biologicals, Lawrenceville, GA, USA) and 5% 1× penicillin and streptomycin mixture (Life Technologies). The enzymes were blocked using fetal bovine serum (FBS), and the muscle extract was treated with Red Blood Cell Lysis Solution to remove erythrocytes. We next performed magnetic labelling by adding buffer containing 5% bovine serum albumin (BSA), 2 mM EDTA, phosphate-buffered saline (PBS) and Satellite Cell Isolation Kit (Miltenyi Biotec), containing a mixture of antibodies specific for non-satellite cells conjugated to magnetic beads. The cell suspension was poured into a column retained in a magnetic field. The unlabelled cells satellite cells flowed through the column while labelled cells are retained within the column. Satellite cells were resuspended in the growth medium [DMEM with 20% FBS, 1% penicillin/streptomycin (P/S), and 2.5 ng/mL of basic fibroblast growth factor] and plated on Matrigel (BD Bioscience, 1:5 dilution in plain DMEM)-coated 6-well plates.

Transcriptome profiling by ribonucleic acid sequencing

Tibialis anterior (TA) muscle was collected from postnatal day 10 SMA ($n = 4$) and unaffected control mice ($n = 5$). Total RNA was quantified via a fluorescence dye-based methodology (RiboGreen) on a Spectramax Gemini XPS plate reader (Molecular Devices, Mountain View, CA) as previously described.[35] RNA integrity was assessed using automated capillary electrophoresis on a Fragment Analyser (Advanced Analytical Technologies, Inc, Santa Clara, CA). Total RNA input of 200 ng was used for library preparation using the TruSeq Stranded mRNA Library Preparation Kit (Illumina, San Diego, CA). Sequencing libraries were quantified by PCR using KAPA Library Quantification Kit for NGS (Kapa, Wilmington, MA) and assessed for size distribution on a Fragment Analyser. Sequencing libraries were pooled and sequenced on a HiSeq 3000 Sequencer (Illumina) after clustering on a cBot2 (Illumina) and using a HiSeq 3000/4000 PE Cluster Kit and HiSeq 3000/4000 SBS Kit (150) cycles for paired-end reads at 75 bp length. Raw sequencing data were demuxed using bcl2fastq2 Conversion Software 2.17 before alignment to the mouse reference genome (mm10) using MapSplice version 2.2.1. Gene read counts against UCSC mouse gene models (obtained on 21 February 2016) were calculated by HTSeq version 0.9.1 with parameters: -m intersection-nonempty -i gene_id -s no. Gene read count normalization and differential expression analysis were performed with DESeq2

version 1.16.1. Sample-level FASTQ files, raw gene counts, and normalized gene counts data are publically available at NCBI Gene Expression Omnibus (Accession # GSE158790). Functional enrichment analysis was performed using the PANTHER Classification System71. Significantly overrepresented gene ontology biological processes at $P < 0.01$ were adjusted using a Bonferroni correction for multiple testing.

Ribonucleic acid isolation and gene expression analysis

Total RNA was isolated from muscle cells using QIAzol (Cat. #79306, Qiagen, Hilden, Germany), and the RNeasy kit (Cat. #74106, Qiagen) was used to purify the RNA according to the manufacturer's instructions (45). One microgram of RNA was converted to cDNA using the High Capacity cDNA Reverse Transcription kit (Cat. #4368813, Thermofisher), following the manufacturer's instructions. Gene expression was determined by qRT-PCR using either TaqMan (Cat. #1725134, Bio-Rad) or SYBR Green reagents (Cat. #1725124, Bio-Rad). TaqMan primers (all Thermo Fisher) were MyoD (TaqMan assay Mm00440387_m1), Myogenin (TaqMan assay Mm00446194_m1), Pax7 (TaqMan assayMm00834079_m1), Pax3 (TaqMan assay Mm00435493_m1), SMN1 (TaqMan assay Mm00488313_m1), myomaker (TaqMan assay Mm00481256_m1), and gusb (TaqMan assay Mm01197698_m1). SYBR primers (all Integrated DNA Technologies) were myomixer (F: 5′-GTT AGA ACT GGT GAC CAG GAG-3′ R: 5′-CCA TCG GGA GCA ATG GAA-3′) and GAPDH (F: 5′-GCA TGG CCT TCC GTG TTC-3′ R: 5′-ATG TCA TCA TAC TTG GCA GGT TTC-3′). Transcript levels were quantified by threshold cycle values using gusb or GAPDH as a control. For cell culture experiments, values were normalized to unaffected cells for each *n*. For animal experiments, values were normalized to the average ΔC_T of all wild-type animals.

Myomaker and myomixer surface expression analysis

Wild-type and SMN-deficient C2C12 cells were plated on coverslips and differentiated for 7 days using DMEM with 2% horse serum. Cells were fixed using 4% paraformaldehyde. Cells were stained for rabbit anti-myomaker (Cat. #ab188300, Abcam, Cambridge, UK) or sheep anti-myomixer (Cat. #AF4580-SP, R&D Systems, Minneapolis, MN, USA) and DAPI. Secondary antibodies rabbit 546 (Cat. #A-11035, Thermofisher) or donkey anti-sheep 557 (Cat. #NL010, R&D Systems) were used. Five images per condition were quantified for each *n*. Within each image, the pixel intensity from 10 cells was measured using ImageJ, and the background signal was subtracted. The average pixel intensity was normalized to wild-type levels for each *n*.

MyoD and myogenin overexpression

Wild-type and SMN-deficient C2C12 cells were plated and after 24 h, transfected with 1 μg MyoD (Cat. #14710, Addgene, Watertown, MA, USA) or myogenin (Cat. #MR227400, Origene Technologies Inc., Rockville, MD, USA) using Lipofectamine 3000 (Thermo Fisher). Cells were collected 48 h after transfection. For differentiation experiments, wild-type and SMN knockdown C2C12 cells were plated. 24 h after plating, cells were simultaneously differentiated and transfected with 1 μg of either MyoD or myogenin. Cells were transfected again 48 h after the first transfection to maintain expression of MyoD or myogenin. Cells were fixed after 5 days of differentiation. Five images per condition were quantified for each *n*. Images were quantified by calculating the fusion index. Values were normalized to wild-type cells for each *n*. Additionally, the number of nuclei per myotube was determined as a measure of myotube maturity.

Proliferation assay

Wild type and SMN knockdown C2C12 cells were plated on coverslips. The next day, cells were transfected with either MyoD or myogenin plasmids. Twenty-four hours after transfection, 10 μM EdU was added to cells, and then 24 h after adding EdU, cells were fixed with 4% paraformaldehyde for 15 min at room temperature. Cells were washed three times with 1× PBS. Fixed cells were permeabilized with 0.5% Triton X-100 in PBS for 20 min at room temperature. Click-iT azide fluor solution (20 μM Azide fluorophore (Cat. #760765, Sigma), 100 mM Tris, 10 mM $CuSO_4$, and 100 mM ascorbic acid diluted in deionized water) was added to cells for 30 min at room temperature with gentle agitation. Cells were washed three times with 100 mM Tris with gentle agitation and counterstained with DAPI. Coverslips were mounted on slides using FluorSave. The percentage of EdU-positive nuclei was determined for five images (a minimum of 865 total nuclei) per condition for each *n*.

Messenger ribonucleic acid stability

Wild-type and SMN knockdown C2C12 cells were plated on a 6-well plate and were differentiated 24 h later. After 48 h of differentiation, 5 μg/mL actinomycin D (Cat. #A9415, Sigma Aldrich) was added to cells. Cells were collected 0, 1, 3, 5, and 8 h after the addition of actinomycin D. RNA was isolated and purified. RNA was reverse transcribed into cDNA. qRT-PCR was used to determine relative mRNA expression over time. ΔC_T values were normalized to the 0 h time point for wild-type and SMN knockdown cells for each *n*.

Chromatin immunoprecipitation

Wild-type C2C12 cells were differentiated for 48 h and then fixed with 1% paraformaldehyde. Chromatin was isolated and purified using the EZ Magna ChIP A/G Kit (Cat. #17-10086, Millipore Sigma) according to the manufacturer's instructions. Anti-SMN antibody (BD Biosciences) was used to immunoprecipitate chromatin. Anti-polymerase II, clone CTD4H8 antibody, and normal mouse IgG were used as a positive and negative control, respectively (Cat. #17-10086, Millipore Sigma). qRT-PCR was used to quantify chromatin. C_T values for each IP were normalized to the C_T value for the same part of the genome (input) for each *n* and then normalized to the IgG IP. We used the 3′ UTR of MyoD and myogenin as negative controls. Fold enrichment of the SMN IP compared with IgG IP were plotted. Primers used to detect chromatin (Integrated DNA Technologies) were MyoD promoter (F: 5′-ACA CTC CTA TTG GCT TGA GGC-3′ R: 5′-GGC GCC CTG GGC TAT TTA TC-3′), myogenin promoter (F: 5′-GAA TCA CAT GTA ATC CAC TGG A-3′ R: 5′-ACA CCA ACT GCT GGG TGC CA-3′), MyoD 3′ UTR (F: 5′-AAC TCT ACG AAC TGG GCG GG-3′ R: 5′-AGG CCT GGG GAA TTC CCT AC-3′) and myogenin 3′ UTR (F: 5′-AGA GGG GAG CCA CCA AAA CT-3′ R: 5′-CAC TTG GCT CCT GCG TCT AA-3′).

MO^{E1v11} antisense oligonucleotide therapeutic

MO^{E1v11} was synthesized as a phosphorodiamidate morpholino oligomer (GeneTools L.L.C.). MO^{E1v11} is a 20-nucleotide oligomer (5′-CUAUAUAUAGUUAUUCAACA-3′).

Production and purification of adeno-associated virus 9-myomixer vector

Viral production was performed as previously described.[29] Briefly, 293 T HEK cells (ATCC CRL 3216) were cultured in four 10-floor cell factories until approximately 85% confluent. Cells were triple transfected with Rep2Cap9 (serotype 2 Rep proteins, serotype 9 capsid proteins), pHelper (adenovirus helper constructs; Stratagene), and scAAV-CBA-myomixer using 25 kDa polyethyleneimine at a molar ratio of 1:1:1. Cells were harvested at 48 h after transfection and suspended in 10 mmol Tris, pH = 8.0, lysed by five freeze–thaw cycles in liquid nitrogen, DNAse treated, and protease treated. CsCl crystals were added to the lysate (0.631 g of CsCl per mL of the lysate) to generate a solution with a density of approximately 1.4 mg/mL. After incubation at 37°C for 45 min, the solution was centrifuged at 3184 *g* in an Eppendorf 5810 R at 4°C. Virus was purified from lysate by three rounds of density gradient centrifugation at an average RCF of 158 000. Vector titres were determined by quantitative real-time PCR. The final fractions were dialyzed against PBS and stored at 4°C until use.

Spinal muscular atrophy mice

The original breeding pairs for the SMA mice (*Smn$^{+/-}$SMN2$^{+/+}$SMNΔ7$^{+/+}$*) on the FVB background were purchased from Jackson Laboratories. The breeding colony was maintained by interbreeding *Smn$^{+/-}$SMN2$^{+/+}$SMNΔ7$^{+/+}$* mice, and offspring were genotyped using PCR assays on tail DNA as previously described.[36]

Antisense oligonucleotide and adeno-associated virus 9-myomixer treatment

Animals were treated with 2 nmol MO^{E1v11} via a single intracerebroventricular injection (ICV) injection on postnatal day 2. Viral delivery of an empty vector or AAV9-myomixer was performed by intravenous injection (1×10^{11} vector genomes) into the superficial vein on postnatal day 2. On postnatal day 11, animals were anaesthetized using isoflurane and sacrificed via decapitation. TA muscles were harvested and flash frozen in liquid nitrogen. Tissues were stored at −80°C until processed.

Histological analysis of tibialis anterior muscle fibre

Mice were transcardially perfused with 4% paraformaldehyde. Distal hind limbs were dissected and postfixed overnight. Hind limb tissues were decalcified, embedded in paraffin, and cross-sectioned at the midpoint of the muscle. All analyses were carried out blinded. Sections (10 μm) were mounted on slides and stained with H&E. Digital images were captured using a Zeiss Axiovert 100 M microscope and analysed with NIH ImageJ software for total myofibre number (original magnification, ×20) and myofibre diameter (original magnification, ×20). Myofibre diameter was determined by measuring the largest diameter of at least 300 neighbouring myofibres per animal.

Righting reflex

Time to right was determined as previously described.[37] Briefly, mice were placed on their back and the time to turn over to their front was measured (maximum 30 s).

Serum creatine kinase assay

Mice were euthanized at postnatal day 12 and 500 μL of blood collected from the right ventricle using a 21-gauge

needle. The serum level of the muscular isoform of creatine kinase (CK-MM) was measured in duplicate, using the CK-MM ELISA Kit (Cat#: MBS705327, MyBioSource, San Diego, CA) according to the manufacturer's instructions.

Statistics

All statistical analyses were carried out using GraphPad Prism v7.05 (GraphPad Software, Inc.). Outliers were determined using Grubbs' test where $\alpha = 0.05$. Normal distribution was assessed using the Shapiro–Wilk normality test and homogeneity of variances was assessed using either an *F* test or a Brown–Forsythe test. Data were analysed using either an unpaired *t*-test (for comparisons with one independent variable and two groups), one-way analysis of variance (ANOVA) (for comparisons with one independent variable and >2 groups), or two-way ANOVA (for comparisons with two independent variables and >2 groups). *Post hoc* analyses were performed using Tukey's multiple comparisons test. Survival curves were analysed using a log-rank (Mantel–Cox) test. A P value <0.05 was considered statistically significant.

Study approval

Animals were housed and treated in accordance with the Animal Care and Use Committee guidelines of the Uniformed Services University of the Health Sciences and the University of Missouri. The Animal Care and Use Committee of the Uniformed Services University and the University of Missouri approved these studies.

Results

Survival motor neuron deficiency reduces expression of membrane fusion proteins

We previously showed that immortalized myoblasts from SMA model mice poorly fuse into myotubes, possibly due to altered myogenic gene expression, compromised cell migration, and membrane fusion.[13] How SMN deficiency alters these pathways remains unclear. In this study, we sought to determine the role of SMN in myoblast membrane fusion, the terminal stage of myotube formation. We transfected C2C12 cells with a lentivirus containing an SMN shRNA. Cells were treated with puromycin, and GFP^+ single cell colonies were selected and expanded. Knockdown of SMN mRNA (55% decrease, $P < 0.0001$) and protein were confirmed through qRT-PCR and western blot analysis, respectively. Further, we showed that using an antisense oligonucleotide designed against the shRNA, we could restore SMN expression 48 h after antisense exposure (51% increase in mRNA compared with SMN knockdown, $P = 0.0003$) (*Figure* 1A). We next investigated the fusion capacity of SMN-deficient cells using a cell mixing assay. We co-plated and differentiated wild-type and SMN-deficient myoblasts labelled with fluorescent trackers and found that SMN-deficient myoblasts fuse with wild-type myoblasts but not with each other, suggesting that SMN-deficient myoblasts have a significantly reduced fusion capacity but are not fusion-incompetent (*Figure* 1B).

Impaired myoblast fusion could be caused by loss of soluble factors that triggers signalling cascades to augment muscle fusion or disruption of dynamic membrane processes mediated by integral membrane proteins.[38,39] To determine if impaired fusion is due to loss of released soluble myogenic factors, we treated SMN-deficient myoblasts with conditioned media from differentiating wild-type myoblasts and found that conditioned media did not initiate fusion of SMN-deficient myoblasts suggesting that compromised fusion is likely due to altered expression or activity of membrane proteins and not the release of soluble myogenic factors (*Figure* 1C). To ensure that conditioned media could induce fusion, we treated wild-type myoblasts with conditioned media from differentiating wild-type myoblasts for 7 days. We found that wild-type myoblasts treated with conditioned media were able to differentiate (*Figure* 1C).

We next sought to determine whether genes involved in the regulation of myoblast fusion are altered when SMN is deficient. We isolated and performed transcriptome profiling of the tibialis anterior (TA) muscle from postnatal day 10 (PND10) wild-type ($n = 5$) and SMA ($n = 4$) model mice (see mRNA-seq quality metrics in the Supporting Information, *Table* S1). At this timepoint, SMA mice are symptomatic. Transcriptome profiling and differential expression analysis observed 19652 features for transcripts expression in either one of the two tissue for comparative analysis (*Figure* 2A). Filtering for these features with log two-fold change >0.585 and FDR < 0.01 resulted in 3940 differentially expressed transcripts between SMA and wild-type skeletal tissue. To focus on discovery of transcripts involved in myoblast fusion function, Protein ANalysis THrough Evolutionary Relationships (PANTHER) revealed an enrichment for myoblast fusion and muscle formation gene ontology with differential expression of four cell adhesion molecules including myomaker (*tmem8c*), a protein required for myoblast fusion and muscle formation (*Figure* 2B–D).[30] It is not surprising that wild-type mice have high expression of myomaker because, at PND10, mice are still undergoing muscle growth and development. Using qRT-PCR, we confirmed that myomaker is reduced by 35% in skeletal muscle of SMA mice at PND10 ($P = 0.0060$) as well as earlier during development at PND4/5 (16% reduction, $P = 0.0329$) (*Figure* 3A,B).

Given that myomaker is required by both cells for fusion to occur, and we found that SMN-deficient myoblasts readily fuse with wild-type myoblasts, myomaker may not be the

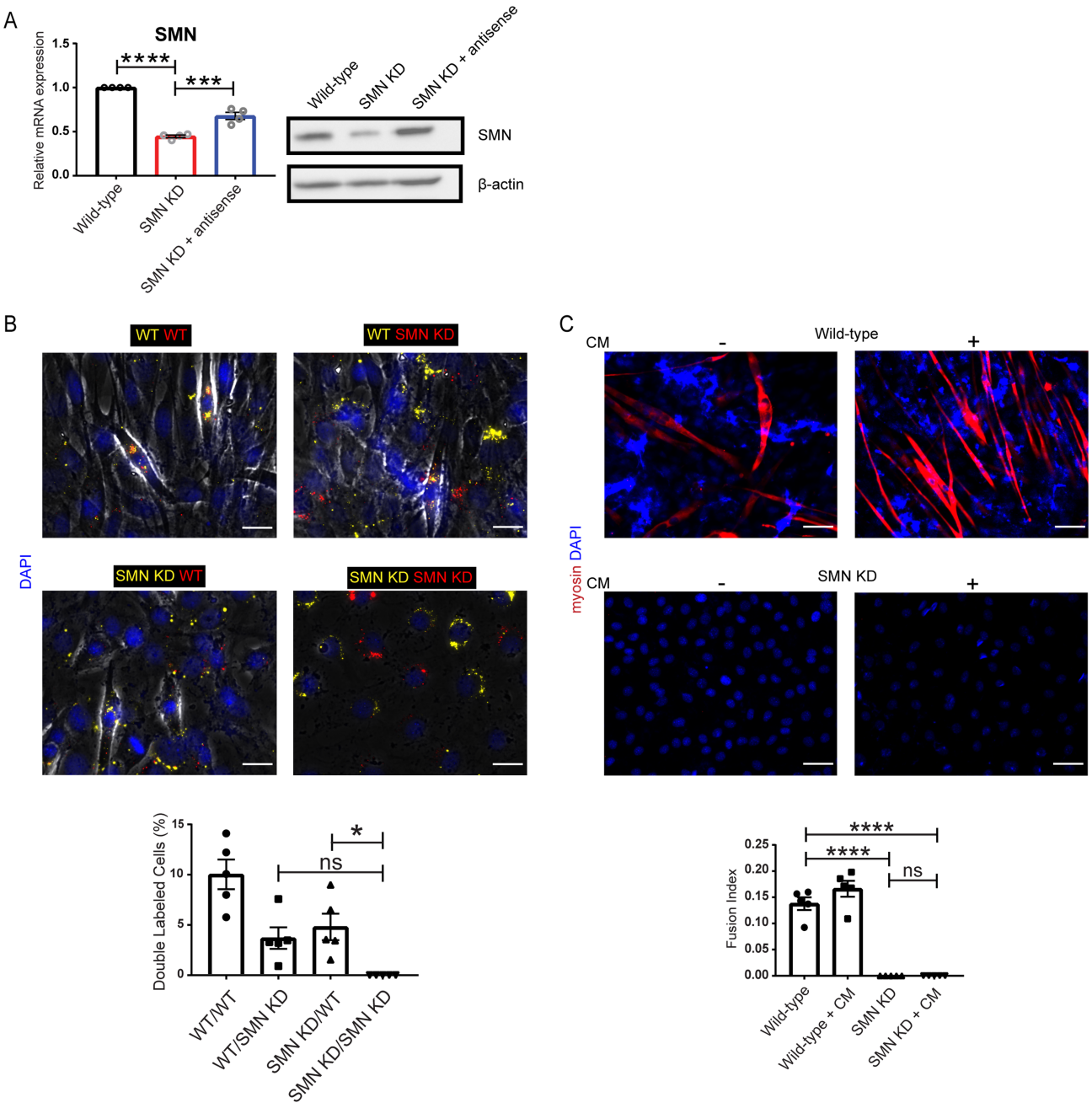

Figure 1 SMN deficiency impairs myoblast fusion. *(A)* SMN mRNA and protein levels in wild-type and SMN knockdown C2C12 cells and SMN knockdown cells (SMN KD) transfected with an antisense oligonucleotide designed to suppress the SMN shRNA. Data were analysed using a one-way ANOVA [$F(2, 9) = 120.1$, $P < 0.0001$] followed by *post hoc* Tukey's test for multiple comparisons (WT vs. SMN KD: $P < 0.0001$; SMN KD vs. SMN KD + ASO: $P = 0.0003$). $n = 4$. *(B)* Wild-type and SMN-deficient C2C12 cells were differentiated for 2 days and then labelled with QTracker 585 (yellow) and 655 (red). After labelling, cells were mixed and differentiated for an additional 5 days. Cells were stained with DAPI (40×; scale bar: 25 μm). The number of double-labelled cells was counted. Data were analysed using a one-way ANOVA [$F(3, 16) = 13.54$, $P = 0.0001$] followed by *post hoc* Tukey's test for multiple comparisons (WT/SMN KD vs. SMN KD/SMN KD: $P = 0.1352$; SMA/WT vs. SMN KD/SMN KD: $P = 0.0369$). $n = 5$. *(C)* Wild-type and SMN-deficient C2C12 cells were treated with conditioned media (CM) from differentiating wild-type C2C12 cells (20×; scale bar: 50 μm) and quantification of fusion index. Data were analysed using a one-way ANOVA [$F(3, 16) = 82.49$, $P < 0.0001$] followed by *post hoc* Tukey's test for multiple comparisons (WT vs. SMN KD: $P < 0.0001$; WT vs. SMN KD + CM: $P < 0.0001$; SMN KD vs. SMN KD + CM: $P > 0.9999$). $n = 5$. All data are represented as mean ± SEM. $^{**}P < 0.01$, $^{***}P < 0.001$, $^{****}P < 0.0001$.

A

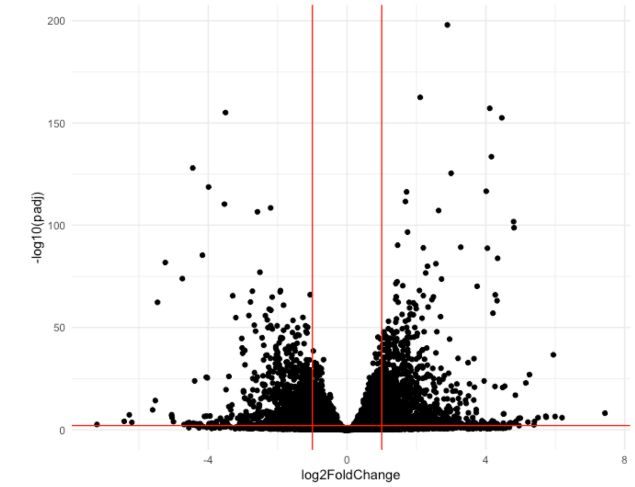

B

Protein Class	% of genes altered
calcium binding protein	3.1
cell adhesion molecule	1
chaperone	0.7
cytoskeletal protein	7.8
defense/immunity protein	2.7
enzyme modulator	12.9
extracellular matrix protein	1.4
hydrolase	13.9
isomerase	1.4
ligase	2.7
lyase	1.7
membrane traffic protein	2.4
nucleic acid binding	8.1
oxidoreductase	6.4
receptor	3.4
signaling molecule	7.1
structural protein	0.7
transcription factor	5.1
transfer/carrier protein	3.1
transferase	8.1
transmembrane receptor regulatory/adaptor protein	0.3
transporter	6.1

C

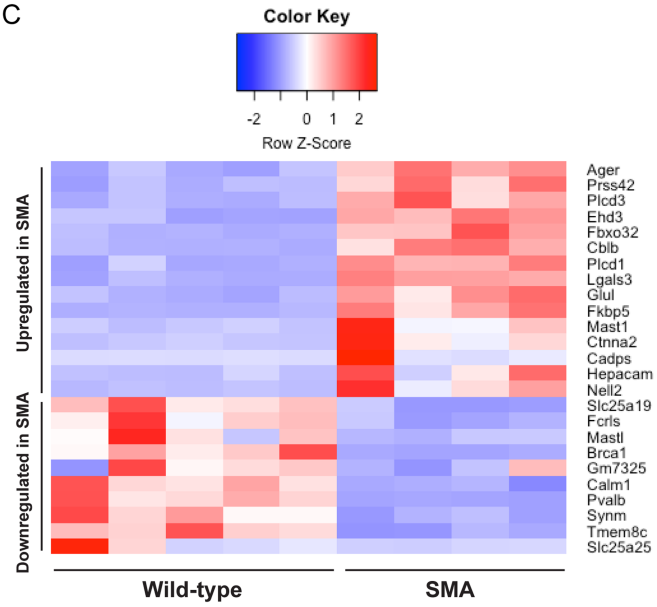

D

Gene		Log2 fold change
Lgals3	Galectin-3	2.11
Ager	Advanced glycosylation end product-specific receptor	1.6
Tmem8c	Myomaker	-1.61
Fcrls	Fc receptor-like S, scavenger receptor	-1.95

Figure 2 Transcriptome analysis of PND10 WT and SMA mouse TA muscle. Analysis was performed on TA muscle from PND10 wild-type (n = 5) and SMNΔ7 (n = 4) mice. A fold change of 1.5 or greater was used as the initial selection criteria. *(A)* Transcript expression profiles between WT and SMA mouse skeletal muscle tissue; 19 652 transcripts from RNA-seq transcriptome profiling as a function of log two-fold change and FDR adjusted P value between SMA and wild type mouse muscle tissue. Red lines represent filter cutoff values for log two-fold change of >0.585 (vertical) and FDR-adjusted P value <0.01 (horizontal). Transcripts with greater expression in SMA as compared with WT are on the right of the plot. *(B)* Protein ANalysis THrough evolutionary relationships (PANTHER) sorts significantly altered genes by protein class. *(C)* Heat map of transcriptome analysis of skeletal muscle from PND10 wild-type and SMNΔ7 mice showing significantly altered calcium binding proteins, cell adhesion molecules, and ligases. *(D)* Cell adhesion molecules significantly altered in skeletal muscle of SMNΔ7 mice.

only fusion molecule deficient in SMA skeletal muscle.[30] Therefore, we examined the expression of a second fusion protein, myomixer, also known as Gm7325, myomerger, and minion, and is only required by one fusing cell.[32–34] We confirmed by qRT-PCR that myomixer expression is significantly reduced in skeletal muscle from both PND4/5 (35% reduction, P = 0.0141) and PND10 (30% reduction, P = 0.0051) SMA mice (*Figure* 3A,B). Because muscle stem cells would drive the repair of injured muscle, we examined the expression of myomaker and myomixer in satellite cells, skeletal muscle stem cells, isolated from the affected tibialis anterior muscle of SMA mice and their wild-type littermates. We found that myomaker and myomixer expression were reduced in satellite cells isolated from PND10 SMA mice compared with wild-type mice (*Figure* 3C).

Myomaker and myomixer expression are usually low in satellite cells and up-regulated during myoblast fusion.[30,32] We next compared the induction of myomaker and myomixer

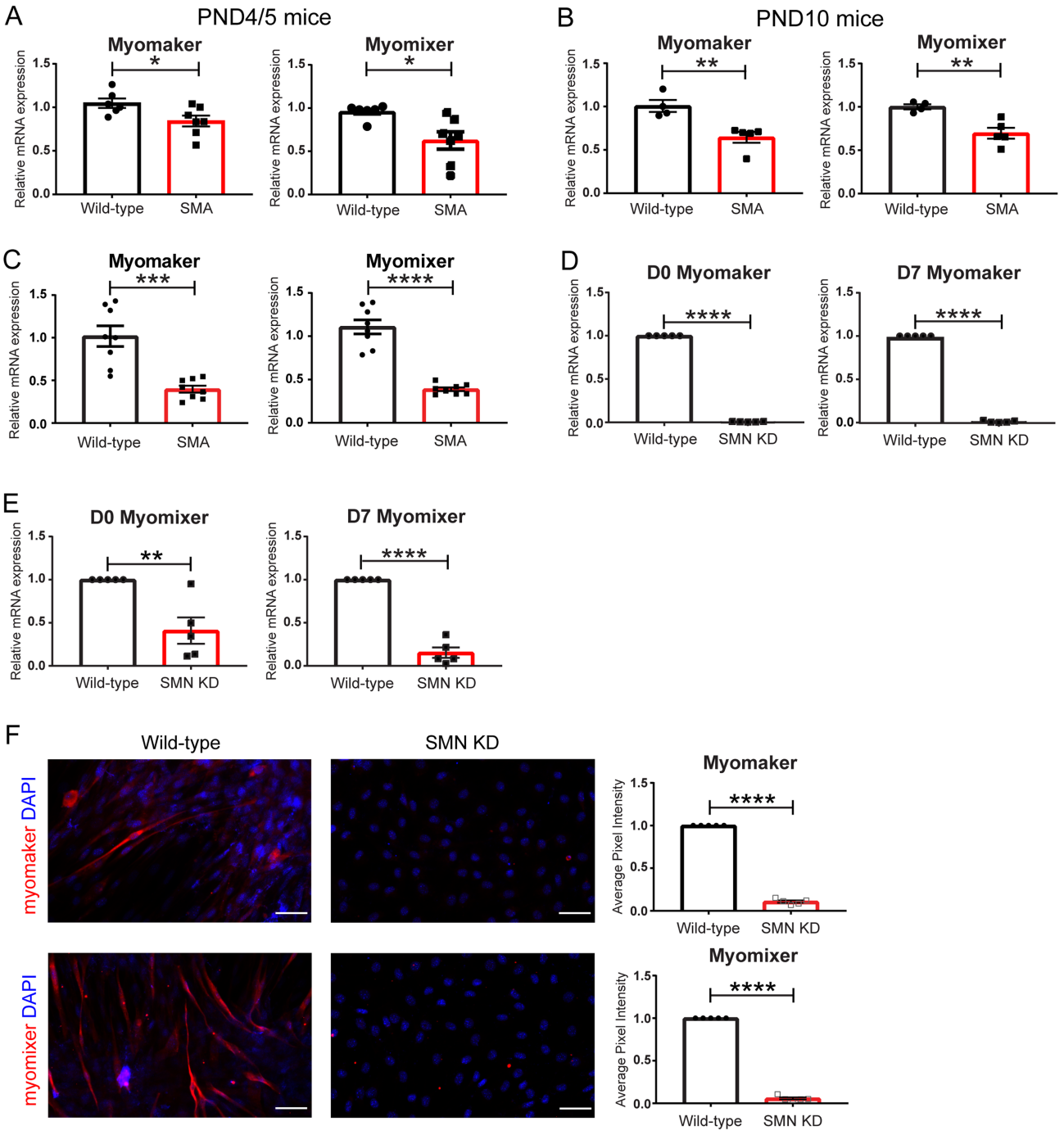

Figure 3 Myomaker and myomixer expression is reduced with SMN deficiency. Myomaker and myomixer mRNA expression in PND4/5 *(A)* and PND10 *(B)* skeletal muscle of wild-type and SMNΔ7 mice. Data were analysed using an unpaired *t*-test (PND4/5 myomaker: $P = 0.0329$; PND4/5 myomixer: $P = 0.0141$; PND10 myomaker: $P = 0.0060$; PND10 myomixer: $P = 0.0051$). $N = 5–7$. *(C)* Myomaker and myomixer mRNA expression in satellite cells isolated from tibialis anterior muscle of wild-type and SMNΔ7 mice. Data were analysed using an unpaired *t*-test (myomaker: $P = 0.0003$; myomixer: $P < 0.0001$). $n = 8$. Myomaker *(D)* and myomixer *(E)* mRNA expression in proliferating (D0) and 7 day differentiated (D7) wild-type and SMN-deficient C2C12 cells. Data were analysed using an unpaired *t*-test (D0 myomaker: $P < 0.0001$; D7 myomaker: $P < 0.0001$; D0 myomixer: $P = 0.0048$; D7 myomixer: $P < 0.0001$). $n = 5$. *(F)* C2C12 cells were differentiated for 7 days, fixed, and immuno-labelled with anti-myomaker or anti- myomixer antibodies and DAPI (20×; scale bar: 50 μm) and quantification of pixel intensity. Data were analysed using an unpaired *t*-test (myomaker: $P < 0.0001$; myomixer: $P < 0.0001$). $n = 5$. All data represented as mean ± SEM. *$P < 0.05$, **$P < 0.01$, ***$P < 0.001$, ****$P < 0.0001$.

DOI: 10.1002/jcsm.12740

during differentiation. We found reduced expression of myomaker (99% reduction, $P < 0.0001$) and myomixer (59% reduction, $P = 0.0048$) in proliferating SMN-deficient myoblasts (*Figure* 3D,E). After 7 days of differentiation, myomaker and myomixer expression remain reduced (99% ($P < 0.0001$) and 85% ($P < 0.0001$) reduction, respectively) in SMN-deficient cells compared with wild-type cells consistent with SMA mice myofibres (*Figure* 3D,E). Given that SMN deficiency did not completely ablate myomaker and myomixer mRNA expression, we looked at the corresponding protein expression in wild-type and SMN-deficient myoblasts. Immunocytochemical analysis revealed markedly reduced expression of myomaker (89% reduction, $P < 0.0001$) and myomixer (94% reduction, $P < 0.0001$) in SMN-deficient C2C12 cells (*Figure* 3F). To determine if restoring SMN rescues myomaker and myomixer expression, we treated SMN-deficient myoblasts with an ASO to the SMN-targeting shRNA to relieve SMN gene repression. Interestingly, we found that while SMN expression was restored 48 h after treatment with the ASO, myomaker expression was significantly increased (204% increase compared with SMN KD levels, $P = 0.0155$), but myomixer expression was not ($P = 0.8506$) 48 h after initiating differentiation (Supporting Information, *Figure* S1a,b). Together, these data suggest that partially restoring SMN expression is sufficient to boost MyoD expression, but the effects on downstream myogenic genes are more limited.

Overexpressing MyoD and myogenin increases myomaker and myomixer expression and partially rescues the fusion deficit of survival motor neuron-deficient myoblasts

Expression of myomaker and myomixer is regulated, in part, by the transcription factors MyoD and myogenin (*Figure* 4A).[40–42] We previously showed that MyoD and myogenin expression are altered in SMN-deficient myoblasts.[13] We first showed that MyoD (95% reduction, $P < 0.0001$) and myogenin (99% reduction, $P < 0.0001$) are reduced in SMN-deficient C2C12 cells after 7 days of differentiation, consistent with our previous findings (*Figure* 4B,C).[13] Restoration of SMN did not fully rescue expression of MyoD (53.5% increase compared with SMN KD, $P = 0.0508$), myogenin (153.6% increase compared with SMN KD, $P = 0.0075$), or Pax7 (11.1% increase compared with SMN KD, $P = 0.9151$), a marker for muscle stem cells (Supporting Information, *Figure* S1c–e). We next examined if restoring MyoD and myogenin is sufficient to increase myomaker and myomixer levels when SMN levels are reduced. Overexpressing MyoD and myogenin for 48 h restored myomaker and myomixer expression in SMN-deficient C2C12 cells (*Figure* 4D). Moreover, overexpressing MyoD or myogenin partially restored fusion of SMN KD myoblasts, with an average of 20% more myotubes with four to seven nuclei compared with SMN KD cells (*Figure* 4E). We verified that the proliferation of wild-type and SMN knockdown C2C12 cells was similar 48 h after transfection with MyoD or myogenin, demonstrating that the observed restoration of fusion was not due to difference in the number of myoblasts (Supporting Information, *Figure* S2). Together, these data indicate that insufficient expression of MyoD and myogenin is at least partially responsible for the reduced expression of myomaker and myomixer in SMN-deficient myoblasts.

We next sought to determine how SMN deficiency alters MyoD and myogenin mRNA expression. We first examined whether SMN deficiency alters MyoD and myogenin mRNA stability. After 48 h of differentiation, we treated wild-type and SMN-deficient C2C12 cells with actinomycin D to inhibit the synthesis of new mRNA. We found no difference in MyoD or myogenin mRNA stability with SMN deficiency (Supporting Information, *Figure* S3a,b). To determine if SMN alters MyoD and myogenin transcription, we immunoprecipitated SMN from wild-type C2C12 cells 48 h after differentiation and probed the bound chromatin for the MyoD and myogenin promoters (*Figure* 4F). We found that SMN interacted with the MyoD ($P = 0.0031$), but not the myogenin ($P = 0.4158$) promoter (*Figure* 4G). As negative controls, we showed that SMN does not associate with the MyoD 3′ UTR ($P = 0.4473$) or the myogenin 3′ UTR ($P = 0.3841$) (Supporting Information, *Figure* S4). Together, these data suggest that SMN may modulate the myogenic program through regulating MyoD transcription.

Restoring survival motor neuron levels in muscle of spinal muscular atrophy mice does not rescue myomaker and myomixer expression

Current treatment options for SMA aim to increase SMN protein levels through increasing expression and correcting splicing of the *SMN2* gene product to slow disease progression.[43] Increasing SMN improves muscle pathology presumably due to slowed denervation, although muscle intrinsic improvements have been described.[9,44] Here, we investigated whether increasing SMN restored myomaker and myomixer expression in SMA model mice; 2 nmol of ASO ($MO^{E1v1.11}$), delivered through intracerebroventricular injection, increased SMN levels through splicing correction, and improved the motor function of SMA model mice.[45] We treated SMA mice with a single dose of ASO ($MO^{E1v1.11}$) at PND2 and harvested TA muscle tissue at PND11 for biochemical analysis. We found ASO treatment resulted in a two-fold increase in full-length SMN expression (*Figure* 5A). However, myomaker (45% less than wild-type, $P < 0.0001$) and myomixer (39% less than wild-type, $P = 0.0002$) expression was not restored in ASO treated SMA mice (*Figure* 5A). These data suggest that postnatal restoration of SMN is insufficient

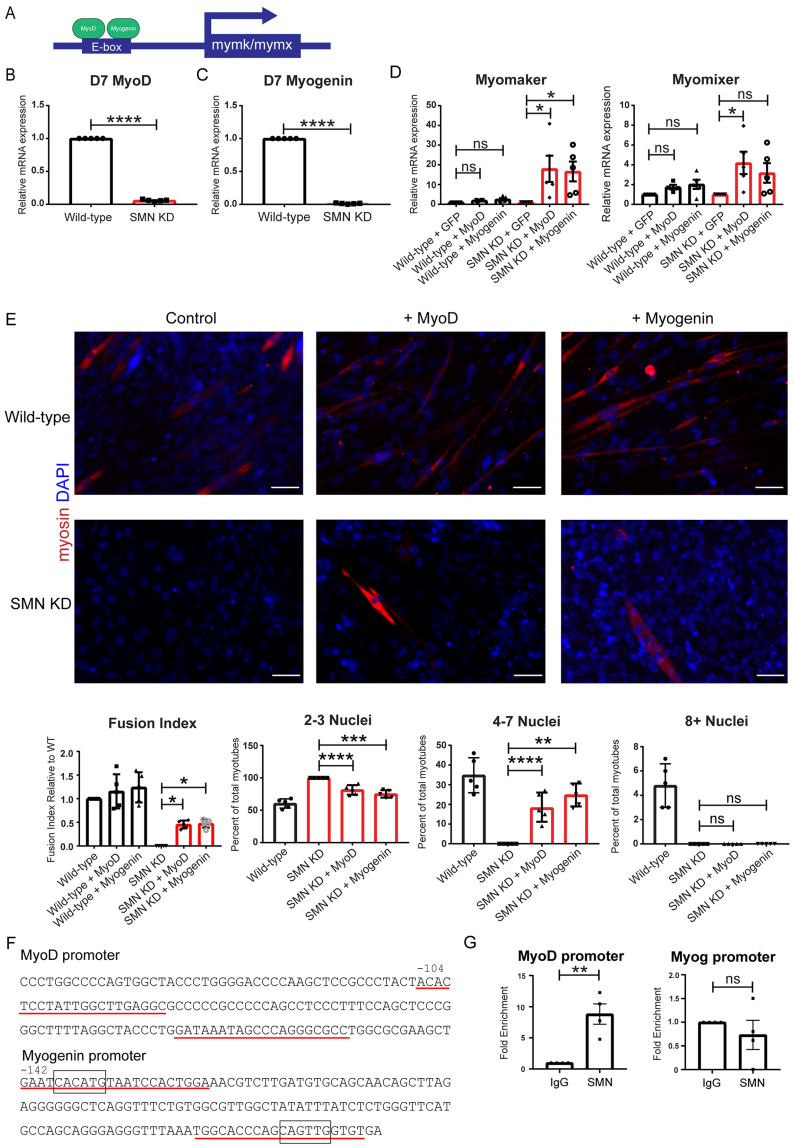

Figure 4 SMN deficiency alters the expression of MyoD and myogenin. *(A)* Schematic showing binding of MyoD and myogenin to E-box elements upstream of the myomaker and myomixer promoters. MyoD *(B)* and myogenin *(C)* mRNA expression in wild-type and SMN-deficient C2C12 cells after 7 days of differentiation. Data were analysed using an unpaired *t*-test (MyoD: $P < 0.0001$; myogenin: $P < 0.0001$). $N = 5$. *(D)* Myomaker and myomixer mRNA expression 48 h after MyoD or myogenin overexpression. Data were analysed using a one-way ANOVA [myomaker: $F(5, 23) = 5.358$, $P = 0.0021$; myomixer: $F(5, 23) = 3.667$, $P = 0.0138$] followed by *post hoc* Tukey's test for multiple comparisons (myomaker: WT vs. WT + MyoD: $P > 0.9999$; WT vs. WT + Myogenin: $P = 0.9996$; SMN KD vs. SMN KD + MyoD: $P = 0.0236$; SMN KD vs. SMN KD + Myogenin: $P = 0.0434$) (myomixer: WT vs. WT + MyoD: $P = 0.9725$; WT vs. WT + Myogenin: $P = 0.8755$; SMN KD vs. SMN KD + MyoD: $P = 0.0251$; SMN KD vs. SMN KD + Myogenin: $P = 0.2222$). $N = 5$. *(E)* MyoD or myogenin were overexpressed in wild-type and SMN-deficient C2C12 cells and differentiated for 5 days. Cells were fixed and stained for myosin and DAPI (20×; scale bar: 50 μM) and quantification of the fusion index and the per cent of total myotubes with 2–3, 4–7, and 8+ nuclei were determined to measure myotube maturity. Fusion index data were analysed using a one-way ANOVA [$F(5, 24) = 28.86$, $P < 0.0001$] followed by *post hoc* Tukey's test for multiple comparisons (WT vs. WT + MyoD: $P = 0.8238$; WT vs. WT + Myogenin: $P = 0.4409$; SMA vs. SMA + MyoD: $P = 0.0185$; SMA vs. SMA + Myogenin: $P = 0.0127$). Myotube maturity data were analysed using a one-way ANOVA [(2–3 nuclei: $F(3, 16) = 38.62$, $P < 0.0001$; 4–7 nuclei: $F(3, 16) = 25.65$, $P < 0.0001$; 8+ nuclei: $F(3, 16) = 36$, $P < 0.0001$] followed by *post hoc* Tukey's test for multiple comparisons (2–3 nuclei SMN KD vs. SMN KD + MyoD: $P < 0.0001$; 2–3 nuclei SMN KD vs. SMN KD + myogenin: $P = 0.0007$; 4–7 nuclei SMN KD vs. SMN KD + MyoD: $P < 0.0001$; 4–7 nuclei SMN KD vs. SMN KD + myogenin: $P = 0.0017$; 8+ nuclei SMN KD vs. SMN KD + MyoD: $P > 0.9999$; 8+ nuclei SMN KD vs. SMN KD + myogenin: $P > 0.9999$). $N = 5$. *(F)* Sequences of the mouse MyoD and myogenin promoters that were probed in ChIP experiments. The primers bound to the sequences underlined in red and E-boxes within these regions are outlined in a black rectangle. The PCR product from the MyoD promoter begins 104 bp upstream of the MyoD start sequence and is 92 bp long. The PCR product from the myogenin promoter begins 142 bp upstream of the myogenin start sequence and is 140 bp long. *(G)* Wild-type C2C12 cells were differentiated for 48 h and fixed. Chromatin co-immunoprecipitated with SMN protein was probed with primers to the MyoD and myogenin promoters. Data were analysed using an unpaired *t*-test (MyoD: $P = 0.0031$; Myogenin: $P = 0.4158$). $n = 4$. All data are represented as mean ± SEM. *$P < 0.05$, **$P < 0.01$, ***$P < 0.001$, ****$P < 0.0001$.

DOI: 10.1002/jcsm.12740

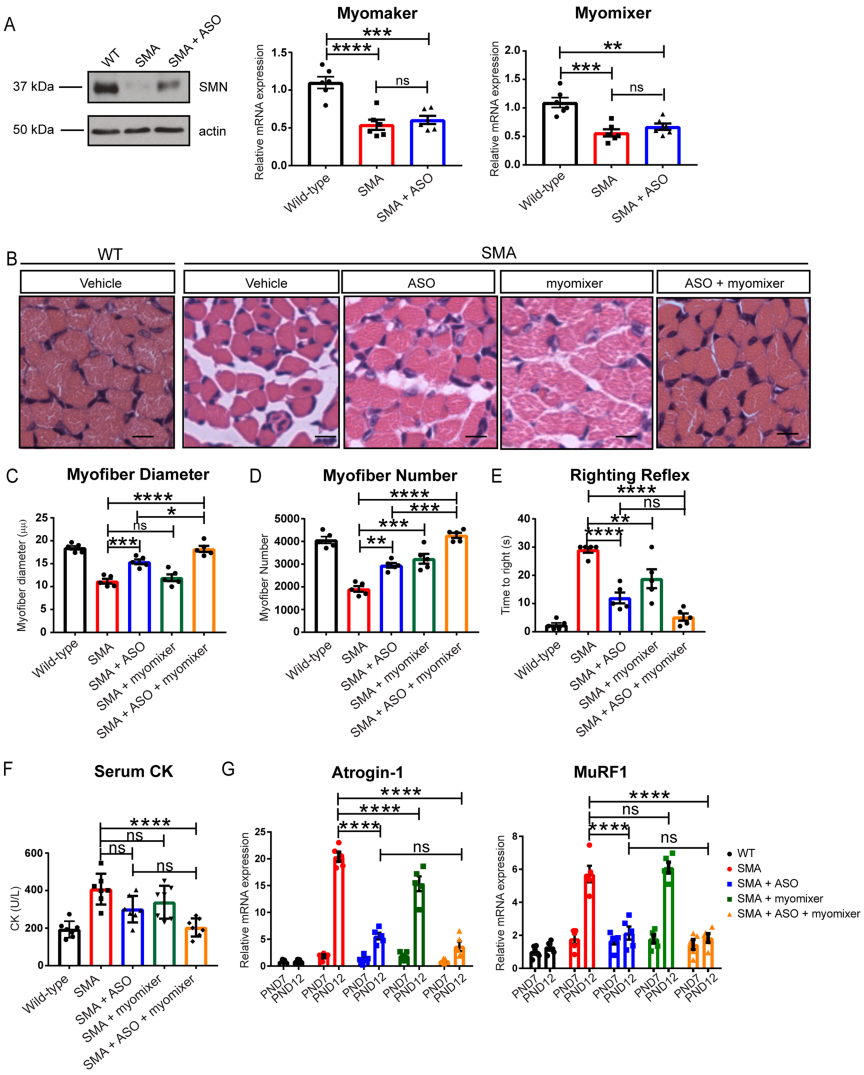

Figure 5 AAV9 delivery of myomixer improves muscle histopathology and motor function of SMNΔ7 mice. *(A)* SMN protein levels in TA muscle from SMA mice treated with an ASO. Myomaker and myomixer mRNA expression in wild-type and SMNΔ7 mice treated with an ASO. Data were analysed using a one-way ANOVA [myomaker: $F(2,15) = 20.84$, $P < 0.0001$; myomixer: $F(2,15) = 16.14$, $P = 0.0002$] followed by *post hoc* Tukey's test for multiple comparisons (myomaker: WT vs. SMA: $P < 0.0001$; WT vs. SMA + ASO: $P = 0.0003$; SMA vs. SMA + ASO: $P = 0.7733$; myomixer: WT vs. SMA: $P = 0.0002$; WT vs. SMA + ASO: $P = 0.0018$; SMA vs. SMA + ASO: $P = 0.5295$). $n = 6$. *(B)* H&E stained muscle cross-sections of TA muscles from wild-type and SMNΔ7 mice treated with an ASO, AAV9-myomixer, or a combination of ASO and AAV9-myomixer. WT and SMA groups were administered an empty vector. Scale bars: 10 μm. Myofibre diameter *(C)*, myofibre number *(D)*, and righting reflex *(E)* of wild-type and SMNΔ7 treated with an ASO, AAV9-myomixer, and an empty vector. Myofibre diameter data were analysed using a one-way ANOVA [$F(4, 20) = 34.15$, $P < 0.0001$] followed by *post hoc* Tukey's test for multiple comparisons (SMA vs. SMA + ASO: $P = 0.0005$; SMA vs. SMA + myomixer: $P = 0.8869$; SMA vs. SMA + ASO + myomixer: $P < 0.0001$; SMA + ASO vs. SMA + ASO + myomixer: $P = 0.0203$). Myofibre number data were analysed using a one-way ANOVA [$F(4, 20) = 41.6$, $P < 0.0001$] followed by *post hoc* Tukey's test for multiple comparisons (SMA vs. SMA + ASO: $P = 0.0059$; SMA vs. SMA + myomixer: $P = 0.0006$; SMA vs. SMA + ASO + myomixer: $P < 0.0001$; SMA + ASO vs. SMA + ASO + myomixer: $P = 0.0006$). Righting reflex data were analysed using a one-way ANOVA [$F(4, 20) = 32.06$, $P < 0.0001$] followed by *post hoc* Tukey's test for multiple comparisons (SMA vs. SMA + ASO: $P < 0.0001$; SMA vs. SMA + myomixer: $P = 0.0089$; SMA vs. SMA + ASO + myomixer: $P < 0.0001$; SMA + ASO vs. SMA + ASO + myomixer: $P = 0.1231$). $n = 5$. *(F)* Serum creatine kinase (CK) levels in wild-type and SMA mice with treatment at postnatal day 12. Data were analysed using a one-way ANOVA [$F(4, 30) = 12.23$, $P < 0.0001$] followed by *post hoc* Tukey's test for multiple comparisons (WT vs. SMA: $P < 0.0001$; WT vs. SMA + ASO + myomixer: $P = 0.9983$; SMA vs. SMA + ASO: $P = 0.0503$; SMA vs. SMA + myomixer: $P = 0.3405$; SMA vs. SMA + ASO + myomixer: $P < 0.0001$; SMA + ASO vs. SMA + ASO + myomixer: $P = 0.0870$). $n = 7$. *(G)* mRNA expression of atrogin-1 and MuRF1 in TA muscle following treatment with ASO and/or AAV9-myomixer. Data were analysed using a two-way ANOVA (atrogin-1: $F(4, 40) = 72.87$, $P < 0.0001$; MuRF1: $F(4, 40) = 22.51$, $P < 0.0001$) followed by *post hoc* Tukey's test for multiple comparisons (Atrogin-1: PND12 SMA vs. PND12 SMA + ASO: $P < 0.0001$; PND12 SMA vs. PND12 SMA + myomixer: $P < 0.0001$; PND12 SMA vs. SMA + ASO + myomixer: $P < 0.0001$; PND12 SMA + ASO vs. PND12 SMA + ASO + myomixer: $P = 0.5571$) (MuRF1: PND12 SMA vs. PND12 SMA + ASO: $P < 0.0001$; PND12 SMA vs. PND12 SMA + myomixer: $P = 0.9954$; PND12 SMA vs. SMA + ASO + myomixer: $P < 0.0001$; PND12 SMA + ASO vs. PND12 SMA + ASO + myomixer: $P = 0.9994$). $N = 7$. All data represented as mean ± SEM. $^*P < 0.05$, $^{**}P < 0.01$, $^{***}P < 0.001$, $^{****}P < 0.0001$.

DOI: 10.1002/jcsm.12740

to correct the fusion deficits of SMA muscle and explain the persistent small muscle size.

Overexpressing myomixer improves histopathology and motor function of spinal muscular atrophy mice

Given that current treatments for SMA prolong lifespan, but only a subset of patients have near normal motor function, we next sought to determine if restoring expression of myomixer improves muscle fibre size and motor function in SMA model mice, alone or in combination with an ASO ($MO^{E1v1.11}$). We treated SMA and control littermates with 1×10^{11} vector genomes of self-complimentary AAV9-myomixer through intravenous injection or a combination of ASO ($MO^{E1v1.11}$) and AAV9-myomixer at PND2 and examined myofibre diameter, and myofibre number at PND11. WT and SMA mice groups were administered 1×10^{11} vector genomes of an empty vector as a control. Myomixer expression was confirmed by western blot analysis, and levels were similar to that of WT mice and persisted through PND40 in mice that were treated with both ASO and AAV9-myomixer (Supporting Information, *Figure* S5). We found that mice treated with ASO had increased myofibre diameter and number as previously reported (*Figure* 5B–D).[45] Delivery of AAV9-myomixer increased the number of myofibres (55% increase, $P = 0.0006$) but had no discernible effect on myofibre diameter ($P = 0.8869$). Interestingly, AAV9-myomixer further increased both myofibre diameter and number when co-administered with ASO over ASO alone (18% ($P = 0.0203$) and 32% ($P = 0.0006$) increase, respectively) (*Figure* 5B–D), even though restoring myomixer levels did not improve gross motor neuron or NMJ histopathology (Supporting Information, *Figure* S6a,b). To determine whether treatment with ASO and AAV9-myomixer affects myofibre maturity, we examined myosin heavy chain (MyHC) isoforms. Consistent with previous reports, we found increased expression of the perinatal form of MyHC and deficiency of an adult MyHC isoform, MyHC IIb in SMA mice (Supporting Information, *Figure* S8). Co-administration of AAV9-myomixer and the ASO reduced expression of the perinatal MyHC and increased expression of MyHC IIb, suggesting the co-treatment synergistically improved some features of muscle maturity.

To determine the functional consequence, if any, of the improved histopathology, we monitored the righting reflex of SMA mice from PND1 to PND10. We found that, consistent with the muscle size data, ectopic myomixer expression improved the righting reflex of SMA mice alone (35% decrease in time to right, $P = 0.0089$) or in combination with ASO (82% decrease in time to right, $P < 0.0001$) (*Figure* 5E). Recent findings demonstrate that serum creatine kinase levels are elevated in SMA mice and patients, even those treated with nusinersen.[20,46,47] These data are consistent with the continued compromise of skeletal muscle, even after increasing SMN levels. We next sought to determine if CK levels are elevated in late stage SMA mice and whether ectopic expression of myomixer suppresses CK induction. We found CK levels were elevated in SMA mice compared with unaffected controls (111% increase, $P < 0.0001$) (*Figure* 5F). SMA mice treated with SMN ASO ($MO^{E1v1.11}$) reduced CK levels (26% decrease, $P = 0.0503$) compared with empty vector-treated mice. AAV9-myomixer treated SMA mice showed retained elevated levels of CK. However, CK levels in SMA mice treated with a combination of ASO ($MO^{E1v1.11}$) and AAV9-myomixer were similar to CK levels in unaffected control mice suggesting muscle membrane integrity was preserved ($P = 0.9983$).

Given that myomixer expression appeared to suppress muscle breakdown, we examined the expression of the atrophy inducing E3 ligases, atrogin-1, and MuRF1. We previously showed that denervation-dependent up-regulation of atrogenes start at postnatal day 11 in SMNΔ7 mice.[14] Here, we found that atrogin-1 and MuRF1 levels remained elevated in TA muscle of SMA mice where myomixer was restored but suppressed in the presence of the ASO (*Figure* 5G). These data suggest that myomixer expression slows muscle fibre loss potentially through suppressing muscle tissue breakdown or facilitating regeneration that outpaces degeneration.

We next looked to see if myomixer alone or in combination with the SMN ASO could prolong the survival of SMA mice. We found that despite the improved motor function, delivery of myomixer alone did not improve the lifespan of SMA mice. However, we observed a modest improvement in survival (28% increase; $P < 0.01$) when myomixer was administered in combination with the SMN targeting ASO (*Figure* 6A). To gain further insight into the mechanism through which myomixer enhanced ASO treatment, we examined the body weight, which serves as a marker of health in SMA mice. We found improved body weight of SMA mice treated with ASO and myomixer compared with cohorts treated with ASO alone at PND20 (54% increase, $P = 0.0003$) and PND30 (63% increase, $P = 0.0018$) (*Figure* 6B). Interestingly, mice treated with the combination of ASO and myomixer showed limited weight gain between PND30 and PND40 (16% increase), while unaffected littermates (WT) continued to gain weight (24% increase).

The loss in body weight by PND40 was coincident with elevated CK levels (137% increase, $P = 0.0002$) in SMA mice treated with ASO and myomixer (*Figure* 6C). Because ASO treated mice died on average at PND31, we examined motor neurons of wild type, ASO and ASO and myomixer treated mice at PND30. We saw dramatic reduction in the number and size of motor neurons in the lumbar (L1–L3) spinal cord of both mice treated with ASO alone (soma size: 26% decrease, $P = 0.0001$; number: 32% decrease, $P < 0.0001$) and those treated with both ASO and myomixer (soma size: 20% decrease, $P = 0.0037$; number: 27% decrease,

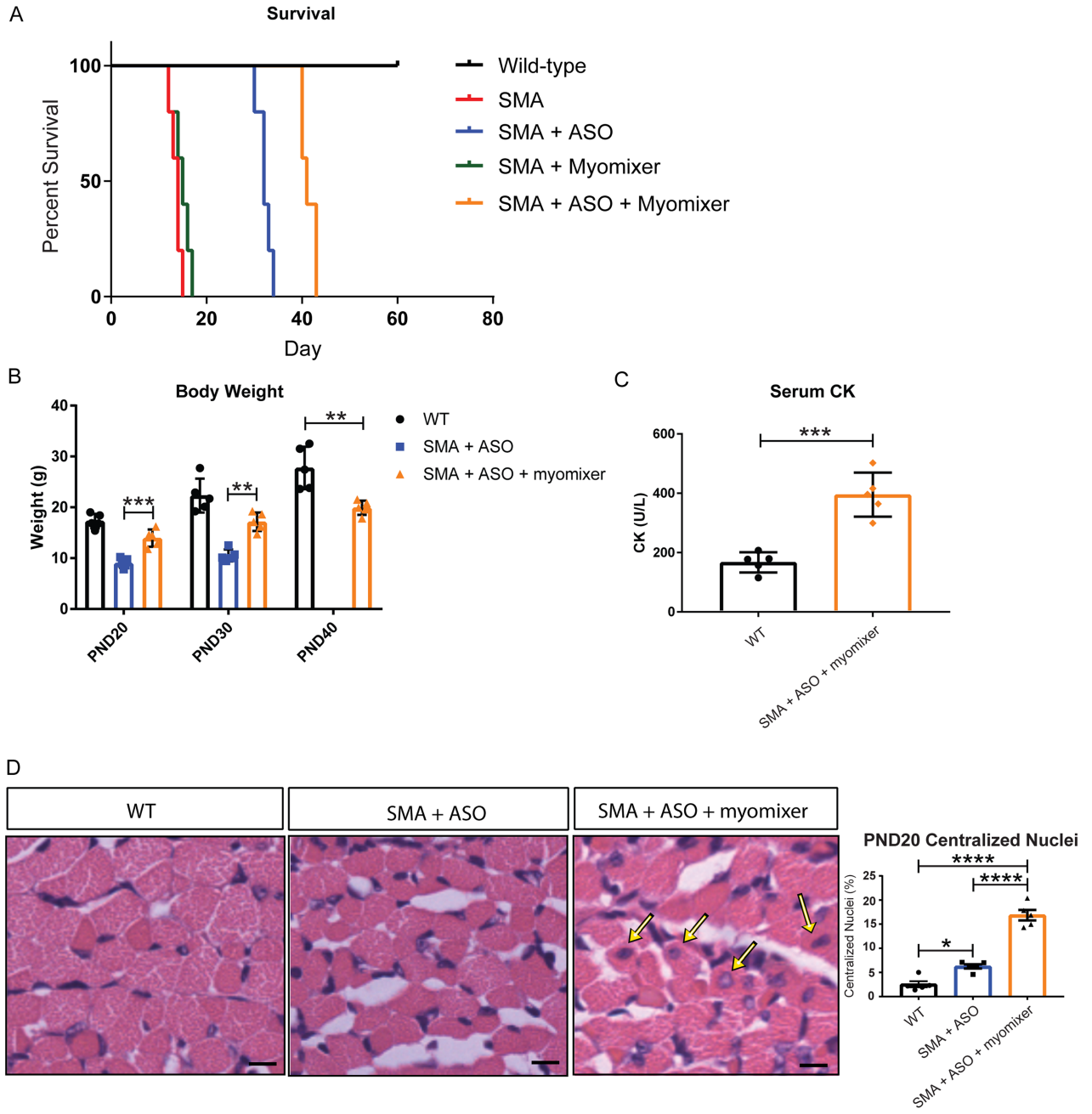

Figure 6 Restoration of myomixer alone does not prolong survival of SMA mice but improves SMA pathology in combination with an SMN-targeting ASO. *(A)* Kaplan–Meier survival plot of wild-type and SMA mice treated with an ASO, AAV9-myomixer, or a combination of ASO and AAV9-myomixer. WT and SMA groups were administered an empty vector. Data were analysed using a log-rank (Mantel–Cox) test ($P < 0.0001$). Median survival was 14 days for SMA mice, 15 days for SMA + myomixer, 32 days for SMA + ASO, and 41 days for SMA + ASO + myomixer. $n = 5$ for each group. *(B)* Body weight was assessed at PND20, 30 and 40 and data at each time point were analysed separately. PND20 data were analysed using a one-way ANOVA [$F(2, 12) = 44.07$, $P < 0.0001$] followed by *post hoc* Tukey's test for multiple comparisons (PND20 SMA + ASO vs. PND20 SMA + ASO + myomixer: $P = 0.0003$). PND30 data were analysed using a one-way ANOVA [$F(2, 12) = 33.11$, $P < 0.0001$] followed by *post hoc* Tukey's test for multiple comparisons (PND30 SMA + ASO vs. PND30 SMA + ASO + myomixer: $P = 0.0018$). PND40 data were analysed using an unpaired *t*-test (PND40 WT vs. PND40 SMA + ASO + myomixer: $P = 0.0041$). $N = 5$. *(C)* Quantification of serum CK levels from PND40 WT and SMA mice treated with ASO and myomixer. Data were analysed using an unpaired *t*-test ($P = 0.0002$). $N = 5$ mice of each cohort. *(D)* H&E-stained transverse sections of TA muscles from a PND20 WT mice and SMA mice treated with either ASO only or ASO and myomixer showing central nuclei (arrows) in the latter. Scale bar: 20 μm. Quantification of central nuclei of TA muscles of PND20 WT, SMA mice treated with ASO and SMA mice treated with ASO and myomixer. Data were analysed using a one-way ANOVA [$F(2, 12) = 93.32$, $P < 0.0001$] followed by *post hoc* Tukey's test for multiple comparisons (WT vs. SMA + ASO: $P = 0.0133$; WT vs. SMA + ASO + myomixer: $P < 0.0001$; SMA + ASO vs. SMA + ASO + myomixer: $P < 0.0001$). $N = 5$ mice from each group. $^*P < 0.05$, $^{**}P < 0.01$, $^{***}P < 0.001$, $^{****}P < 0.0001$.

DOI: 10.1002/jcsm.12740

$P = 0.0008$), suggesting that the motor neuron degeneration occurred around PND30 and triggered muscle atrophy in both treatment groups (Supporting Information, *Figure* S7a). We found increased induction of both atrogin-1 and MuRF1 at PND30 in the TA of ASO only (MuRF1: 332% increase, $P < 0.0001$; atrogin-1: 774% increase, $P < 0.0001$) and ASO and myomixer treated mice (MuRF1: 358% increase, $P < 0.0001$; atrogin-1: 749% increase, $P < 0.0001$) (Supporting Information, *Figure* S7b), consistent with the induction of denervation-dependent atrophy.

The presence of centralized nuclei is a surrogate marker of muscle regeneration. We thus quantified the number of centralized nuclei in SMA treated mice and unaffected controls. We found that mice treated with the combination of ASO and myomixer had elevated centralized nuclei compared with unaffected controls (561% increase, $P < 0.0001$) and SMA mice treated with ASO only (169% increase, $P < 0.0001$) at PND20 (*Figure* 6D). Together, these findings confirm that SMA muscle pathology and motor function can be improved by targeting skeletal muscle in combination with an SMN-enhancing treatment that slows motor neuron loss.

Discussion

Spinal muscular atrophy patients have fewer myofibres and smaller muscles which could be due in part to the reduced fusion of SMN-deficient muscle cells during development or denervation-dependent atrophy.[48] Our previous findings suggested that SMN deficiency impaired myoblast fusion potentially through impaired myogenic gene expression, cell migration, and membrane fusion.[13] It remained unclear how loss of SMN impaired these key features of myotube formation. In the present study, we sought to identify the mechanism through which SMN deficiency impairs myoblast fusion and determine whether myoblast fusion could be targeted to improve muscle pathology and motor function in SMA mice.

Survival motor neuron-deficient myoblasts lack key fusion proteins

We found that SMN-deficient myoblasts and muscle fibres and satellite cells from SMA model mice have reduced expression of myomaker and myomixer, two proteins that are essential for myoblast fusion. Reduction of myomaker and myomixer may explain previous findings that SMA mice have fewer and smaller muscle fibres and why SMN-deficient myoblasts and satellite cells fuse poorly.[8,13,19,49,50] SMN deficiency also alters the expression of the genes responsible for initiating the myogenic program, MyoD and myogenin.[10] Partial restoration of endogenous SMN did not restore the myogenic programming indicating that current treatments may not be sufficient to ameliorate muscle intrinsic defects. Ectopic overexpression of MyoD and myogenin restores myomaker and myomixer expression in myoblasts and partially rescues myoblast fusion even when SMN is reduced suggesting these genes act downstream of SMN in regulating myomaker and myomixer expression.

Survival motor neuron alters muscle fusion through MyoD

We showed here that SMN binds to the promoter region of MyoD suggesting that SMN may directly or indirectly regulate myogenic differentiation at the level of MyoD transcription. We did not detect SMN at the myogenin promoter, indicating that reduced myogenin expression is likely due to reduced expression of MyoD, at an earlier stage of myoblast differentiation (reviewed in Faralli and Dilworth[51]). Consistent with this, we showed that restoring myogenin partially rescues the fusion deficit of SMN-deficient myoblasts. Because SMN-deficient myoblasts readily fuse with wild-type myoblasts and myomaker is needed on both cells to fuse, it is likely that while not optimal, SMN-deficient myoblasts had sufficient levels of myomaker to remain fusion competent. We therefore focused our *in vivo* studies on assessing if myomixer overexpression could improve SMA muscle pathology. We show here that ectopic expression of myomixer slowed myofibre loss and improved motor function in a severe mouse model of SMA. To our knowledge, this is one of a few studies that demonstrate that myoblast fusion can be targeted *in vivo* to improve motor function. While this manuscript was in preparation, it was reported that deletion of myomaker improves the histopathology and motor function of Duchene Muscular Dystrophy mice.[52] These seemingly conflicting findings suggest that fusion proteins may have differing effects depending on the disease mechanism and state of the existing muscle fibres. Nevertheless, we showed here that myomixer overexpression enhances the effects of an SMN ASO ($MO^{E1v1.11}$) that corrects *SMN2* splicing on muscle histopathology and motor function in SMA mice. Our data indicate that myoblast fusion may be a potential SMN-independent mechanism that can be targeted in combination with current therapies to improve SMA pathology.

Improving muscle size and function is a therapeutic strategy for treating spinal muscular atrophy

Current treatments for SMA markedly improve lifespan with a small subset of patients having improvements in motor function, especially with early intervention.[25–28,53] Nevertheless, profound functional deficits remain, with many patients failing to reach normal motor milestones. While

slowing motor neuron loss is central to improving the SMA pathology, SMN-independent treatments, such as those that target muscle, may enhance the efficacy of splicing modifiers and SMN gene therapy. Muscle has long been considered a tissue that could be targeted to improve motor function in SMA.[9,17,49,54–56] We and others have shown that SMA muscles are small and undergo denervation dependent atrophy during disease progression.[10,14] Some drugs that target skeletal muscle in current clinical trials aim to improve muscle growth by inhibiting myostatin (SRK-015) (NCT03921528)[57] or sensitize the troponin complex to lower the threshold for muscle contractility (CK-2127107) (NCT02644668).[58] While many of these treatment strategies show promising early results, better understanding of the growth and contractile capacity of SMA muscle is sorely needed.

Conclusions

In this study, we identified myoblast fusion as a novel mechanism to improve muscle pathology in SMA that could enhance current approved treatments. We show that muscle pathology and motor function can be improved with ectopic delivery of a muscle fusion protein in combination with an ASO that boosts SMN expression. Given that the focus of the current study was to assess the gross motor and pathological improvements of SMN-deficient muscle, it remains unclear if the improved motor function observed when myomixer is overexpressed in combination with an ASO results from increased muscle size or enhanced excitation-contraction coupling. More detailed follow-up analyses to tease out the individual contributions of muscle satellite cells and pre-existing fibres will need to be performed to address when and where the fusion protein is acting. Also, while we did not observe gross improvement in the NMJ morphology, it is possible that restoring myomixer expression altered the electrophysiological profile of the NMJ or the threshold for muscle contraction. Nevertheless, the results from this initial study strongly suggest that compounds or biologics that drive muscle fibre growth through myoblast fusion could offer an additional therapeutic tool to improve the clinical outcomes of SMA patients.

Acknowledgements

We thank Dr. Leonid Chernomordik (National Institutes of Health) for fruitful discussions. This work was supported by grants from CureSMA, National Institute of Neurological Disorders and Stroke (1R01NS119594) (to B.G.B.) and the Missouri Spinal Cord Injury and Disease Research Program (to C.L.L.). The authors certify that they comply with the ethical guidelines for publishing in the *Journal of Cachexia, Sarcopenia and Muscle*.[59]

Online supplementary material

Additional supporting information may be found online in the Supporting Information section at the end of the article.

Figure S1. Restoration of SMN does not fully rescue myogenic programming. SMN knockdown C2C12 cells were transfected with an antisense oligonucleotide designed to suppress the SMN shRNA and maintained for 48 hours. Cells were collected 48 hours after initiating differentiation and mRNA was isolated and converted to cDNA. mRNA expression of myomaker (*A*), myomixer (*B*), Pax7 (*C*), MyoD (*D*), and myogenin (*E*) in wild-type, SMN knockdown cells, and SMN knockdown cells transfected with the antisense oligonucleotide. Myomaker mRNA data were analysed using a one-way ANOVA ($F(2,9) = 26.93$, $p = 0.0002$) followed by *post hoc* Tukey's test for multiple comparisons (WT vs. SMN KD: $p = 0.0001$; WT vs. SMN KD + ASO: $p = 0.0144$; SMN KD vs. SMN KD + ASO: $p = 0.0115$). $n = 4$. Myomixer mRNA data were analysed using a one-way ANOVA ($F(2,9) = 13.98$, $p = 0.0017$) followed by followed by *post hoc* Tukey's test for multiple comparisons (WT vs. SMN KD: $p = 0.0024$; WT vs. SMN KD + ASO: $p = 0.0052$; SMN KD vs. SMN KD + ASO: $p = 0.8506$). $n = 4$. Pax7 mRNA data were analysed using a one-way ANOVA ($F(2,12) = 3.518$, $p = 0.0628$). $n = 5$. MyoD mRNA data were analysed using a one-way ANOVA ($F(2,9) = 13.63$, $p = 0.0019$) followed by *post hoc* Tukey's test for multiple comparisons (WT vs. SMN KD: $p = 0.0014$; WT vs. SMN KD + ASO: $p = 0.0870$; SMN KD vs. SMN KD + ASO: $p = 0.0508$). $n = 4$. Myogenin mRNA data were analysed using a one-way ANOVA ($F(2,9) = 50.02$, $p < 0.0001$) followed by *post hoc* Tukey's test for multiple comparisons (WT vs. SMN KD: $p < 0.0001$; WT vs. SMN KD + ASO: $p = 0.0001$; SMN KD vs. SMN KD + ASO: $p = 0.0975$). $n = 4$. $^{*}p < 0.05$, $^{**}p < 0.01$, $^{***}p < 0.001$, $^{****}p < 0.0001$.

Figure S2. Proliferation of wild-type and SMN knockdown C2C12 cells transiently expressing MyoD or myogenin. (A) Wild-type and SMN knockdown C2C12 cells were plated on coverslips and transfected with either MyoD or myogenin. 24 hours after transfection, 10 μM EdU was added. Cells were fixed 24 hours after the addition of EdU. Coverslips were incubated with Click-iT azide fluor solution to reveal EdU labeling and counterstained with DAPI. The percentage of EdU-positive nuclei was determined for five images and a minimum of 865 nuclei per condition for each n. Data was analysed using a one-way ANOVA ($F(5,18) = 1.226$, $p = 0.3372$). $n = 4$.

Figure S3. MyoD and myogenin mRNA stability does not change with SMN-deficiency. Wild-type and SMN knockdown

cells were differentiated for 48 hours and then treated with actinomycin D to inhibit transcription. Cells were collected 0, 1, 3, 5, and 8 hours after the addition of actinomycin D and mRNA was isolated and converted to cDNA. MyoD (*A*) and myogenin (*B*) mRNA expression following the addition of actinomycin D. $n = 5$.

Figure S4. SMN does not associate with the MyoD or myogenin (myog) 3′ untranslated regions (UTRs). Wild-type C2C12 cells were differentiated for 48 hours and then fixed. Chromatin co-immunoprecipitated with SMN protein was probed with primers to the MyoD (A) and myogenin (B) 3′ UTRs. Data were analysed using an unpaired *t*-test (MyoD 3′ UTR: $p = 0.4473$; Myog 3′ UTR: $p = 0.3841$). $n = 4$. All data are represented as mean ± SEM.

Figure S5. Expression of myomixer in tibialis anterior (TA) muscles from WT and SMA mice following injection of ASO and AAV9-myomixer. (A) SMA mice were administered ASO through intracerebroventricular injection and AAV9-myomixer through intravenous injection at postnatal day 2 and skeletal muscle was harvested at 2, 5, 10, 20, 30, and 40 days post-injection. Skeletal muscle tissue lysates were resolved by SDS-PAGE and transferred to PVDF membranes. Membranes were blocked in 5% milk and probed with a sheep anti-myomixer antibody (R&D Systems), goat anti-sheep secondary, and mouse anti-β-actin.

Figure S6. Myomixer does not improve motor neuron and neuromuscular junction histopathology. (A) Mice were transcardially perfused with 4% paraformaldehyde at postnatal day 12 and lumbar spinal cords dissected and postfixed overnight. Paraffin-embedded lumbar spinal cord was serially sectioned in 10-μm steps, mounted on slides, and stained with Nissl stain. Scale bars: 100 μm. Images of 15 contiguous sections, 150 μm apart (original magnification, ×20) were analysed with NIH ImageJ software. The diameter and number of all neurons greater than 25 μm in the region below a line drawn horizontally at the level of the spinal canal were determined. Motor neuron count data were analysed using a one-way ANOVA ($F(2,57) = 25.75$, $p < 0.0001$) followed by *post hoc* Tukey's test for multiple comparisons (WT vs. SMA: $p < 0.0001$; SMA vs. SMA + myomixer: $p = 0.8325$). Motor neuron size data were analysed using a one-way ANOVA ($F(2,57) = 8.111$, $p = 0.0008$) followed by *post hoc* Tukey's test for multiple comparisons (WT vs. SMA: $p = 0.0006$; SMA vs. SMA + myomixer: $p = 0.4277$). (B) NMJ size and innervation were analysed by confocal imaging was performed using a Zeiss LSM 510 META (Carl Zeiss Inc.; Thornwood, NY) microscope and Z-stacked images were taken at 1 μm intervals and deconvoluted using MetaMorph® Imaging System software. Analysis was done on the affected longissimus capitis muscle by blinded counts for a minimum of 5 fields of view per muscle type from $n = 5$ animals per treatment. NMJ surface area data were analysed using a one-way ANOVA ($F(4,245) = 271.1$, $p < 0.0001$) followed by *post hoc* Tukey's test for multiple comparisons (SMA vs. SMA + ASO: $p < 0.0001$; SMA vs. SMA + myomixer: $p = 0.8937$; SMA vs. SMA + ASO + myomixer: $p < 0.0001$; SMA + ASO vs. SMA + ASO + myomixer: $p = 0.0081$). Statistical comparisons of fully innervated NMJ percentages are presented. End plate innervation data were analysed using a one-way ANOVA ($F(4,245) = 25.45$, $p < 0.0001$) followed by *post hoc* Tukey's test for multiple comparisons (SMA vs. SMA + ASO: $p = 0.0013$; SMA vs. SMA + myomixer: $p = 0.9582$; SMA vs. SMA + ASO + myomixer: $p < 0.0001$; SMA + ASO vs. SMA + ASO + myomixer: $p = 0.8032$). $^{**}p < 0.01$, $^{***}p < 0.001$, $^{****}p < 0.0001$.

Figure S7. Myomixer does not improve motor neuron histopathology or reduce atrogene expression at PND30. (A) Mice were transcardially perfused with 4% paraformaldehyde at postnatal day 30 and lumbar spinal cords dissected and postfixed overnight. Paraffin-embedded lumbar spinal cord was serially sectioned in 10-μm steps, mounted on slides, and stained with Nissl stain. Scale bars: 100 μm. Images of 15 contiguous sections, 150 μm apart (original magnification, ×20) were analysed with NIH ImageJ software. The diameter and number of all neurons greater than 25 μm in the region below a line drawn horizontally at the level of the spinal canal were determined. Motor neuron count data were analysed using a one-way ANOVA ($F(2,57) = 12.08$, $p < 0.0001$) followed by *post hoc* Tukey's test for multiple comparisons (WT vs. SMA + ASO: $p < 0.0001$; WT vs. SMA + ASO + myomixer: $p = 0.0008$; SMA + ASO vs. SMA + ASO + myomixer: $p = 0.7632$). Motor neuron size data were analysed using a one-way ANOVA ($F(2,57) = 10.58$, $p < 0.0001$) followed by *post hoc* Tukey's test for multiple comparisons (WT vs. SMA + ASO: $p = 0.0001$; WT vs. SMA + ASO + myomixer: $p = 0.0037$; SMA + ASO vs. SMA + ASO + myomixer: $p = 0.5717$). (B) mRNA was extracted from TA muscle of PND30 mice following treatment with ASO and/or AAV9-myomixer. mRNA was converted to cDNA and cDNA was used in qRT-PCR to quantify expression of atrogin-1 and MuRF1. Atrogin-1 mRNA data were analysed using a one-way ANOVA ($F(2,12) = 47.13$, $p < 0.0001$) followed by *post hoc* Tukey's test for multiple comparisons (WT vs. SMA + ASO: $p < 0.0001$; WT vs. SMA + ASO + myomixer: $p < 0.0001$; SMA + ASO vs. SMA + ASO + myomixer: $p = 0.8149$). MuRF1 mRNA data were analysed using a one-way ANOVA ($F(2,12) = 90.36$, $p < 0.0001$) followed by *post hoc* Tukey's test for multiple comparisons (WT vs. SMA + ASO: $p < 0.0001$; WT vs. SMA + ASO + myomixer: $p < 0.0001$; SMA + ASO vs. SMA + ASO + myomixer: $p = 0.9239$). $n = 5$ animals per group. $^{***}p < 0.001$, $^{****}p < 0.0001$.

Figure S8. Expression of myosin heavy chain (MyHC) isoforms in SMA mice treated with ASO and/or AAV9-myomixer. SMA mice were treated with either ASO, AAV9-myomixer, or both ASO and AAV9-myomixer and tibialis anterior muscle was harvested at PND12. RT-PCR was performed to examine gene expression of (A) embryonic MyHC, (B) perinatal MyHC, (C)

MyHC I, (D) MyHC IIa, (E) MyHC IIb, and (F) MyHC IIx. Embryonic MyHC data was analysed using a one-way ANOVA ($F(4,20) = 1.409$, $p = 0.2672$). Perinatal MyHC data was analysed using a one-way ANOVA ($F(4,20) = 18.61$, $p < 0.0001$) followed by *post hoc* Tukey's multiple comparisons test (SMA vs. SMA + ASO: $p = 0.0013$; SMA vs. SMA + myomixer: $p < 0.0001$; SMA vs. SMA + ASO + myomixer: $p < 0.0001$; SMA + ASO vs. SMA + ASO + myomixer: $p = 0.1556$). MyHC I data was analysed using a one-way ANOVA ($F(4,20) = 9.905$, $p = 0.0001$) followed by *post hoc* Tukey's multiple comparisons test (SMA vs. SMA + ASO: $p = 0.6294$; SMA vs. SMA + myomixer: $p > 0.9999$; SMA vs. SMA + ASO + myomixer: $p = 0.9040$; SMA + ASO vs. SMA + ASO + myomixer: $p = 0.9823$). MyHC IIa data was analysed using a one-way ANOVA ($F(4,20) = 4.380$, $p = 0.0105$) followed by *post hoc* Tukey's multiple comparisons test (SMA vs. SMA + ASO: $p = 0.1665$; SMA vs. SMA + myomixer: $p = 0.7493$; SMA vs. SMA + ASO + myomixer: $p = 0.2886$; SMA + ASO vs. SMA + ASO + myomixer: $p = 0.9971$). MyHC IIb data was analysed using a one-way ANOVA ($F(4,20) = 28.33$, $p < 0.0001$) followed by *post hoc* Tukey's multiple comparisons test (SMA vs. SMA + ASO: $p = 0.0006$; SMA vs. SMA + myomixer: $p = 0.1908$; SMA vs. SMA + ASO + myomixer: $p < 0.0001$; SMA + ASO vs. SMA + ASO + myomixer: $p = 0.0116$). MyHC IIx data was analysed using a one-way ANOVA ($F(4,20) = 3.518$, $p = 0.0249$) followed by *post hoc* Tukey's multiple comparisons test (SMA vs. SMA + ASO: $p = 0.0849$; SMA vs. SMA + myomixer: $p = 0.1920$; SMA vs. SMA + ASO + myomixer: $p = 0.6953$; SMA + ASO vs. SMA + ASO + myomixer: $p = 0.6171$). $n = 5$ animals per group. $^{*}p < 0.05$, $^{**}p < 0.01$, $^{***}p < 0.001$, $^{****}p < 0.0001$.

Table S1. Sequencing quality metrics for mRNA-seq transcriptome analysis of wild type and SMA skeletal muscle tissue.

Conflict of interest

The authors declare no conflicts of interest.

References

1. Lefebvre S, Burglen L, Reboullet S, Clermont O, Burlet P, Viollet L, et al. Identification and characterization of a spinal muscular atrophy-determining gene. *Cell* 1995;**80**:155–165.
2. Monani UR. Spinal muscular atrophy: a deficiency in a ubiquitous protein; a motor neuron-specific disease. *Neuron* 2005;**48**: 885–896.
3. Lorson CL, Hahnen E, Androphy EJ, Wirth B. A single nucleotide in the SMN gene regulates splicing and is responsible for spinal muscular atrophy. *Proc Natl Acad Sci U S A* 1999;**96**:6307–6311.
4. Monani UR, Lorson CL, Parsons DW, Prior TW, Androphy EJ, Burghes AH, et al. A single nucleotide difference that alters splicing patterns distinguishes the SMA gene SMN1 from the copy gene SMN2. *Hum Mol Genet* 1999;**8**:1177–1183.
5. Coovert DD, Le TT, McAndrew PE, Strasswimmer J, Crawford TO, Mendell JR, et al. The survival motor neuron protein in spinal muscular atrophy. *Hum Mol Genet* 1997;**6**:1205–1214.
6. Pellizzoni L, Kataoka N, Charroux B, Dreyfuss G. A novel function for SMN, the spinal muscular atrophy disease gene product, in pre-mRNA splicing. *Cell* 1998;**95**: 615–624.
7. Burghes AH, Beattie CE. Spinal muscular atrophy: why do low levels of survival motor neuron protein make motor neurons sick? *Nat Rev Neurosci* 2009;**10**:597–609.
8. Arnold AS, Gueye M, Guettier-Sigrist S, Courdier-Fruh I, Coupin G, Poindron P, et al. Reduced expression of nicotinic AChRs in myotubes from spinal muscular atrophy I patients. *Lab Invest* 2004;**84**:1271–1278.
9. Bowerman M, Murray LM, Boyer JG, Anderson CL, Kothary R. Fasudil improves survival and promotes skeletal muscle development in a mouse model of spinal muscular atrophy. *BMC Med* 2012;**10**:24.
10. Boyer JG, Deguise MO, Murray LM, Yazdani A, De Repentigny Y, Boudreau-Lariviere C, et al. Myogenic program dysregulation is contributory to disease pathogenesis in spinal muscular atrophy. *Hum Mol Genet* 2014;**23**:4249–4259.
11. Boyer JG, Ferrier A, Kothary R. More than a bystander: the contributions of intrinsic skeletal muscle defects in motor neuron diseases. *Front Physiol* 2013;**4**:356.
12. Boyer JG, Murray LM, Scott K, De Repentigny Y, Renaud JM, Kothary R. Early onset muscle weakness and disruption of muscle proteins in mouse models of spinal muscular atrophy. *Skelet Muscle* 2013;**3**:24.
13. Bricceno KV, Martinez T, Leikina E, Duguez S, Partridge TA, Chernomordik LV, et al. Survival motor neuron protein deficiency impairs myotube formation by altering myogenic gene expression and focal adhesion dynamics. *Hum Mol Genet* 2014;**23**:4745–4757.
14. Bricceno KV, Sampognaro PJ, Van Meerbeke JP, Sumner CJ, Fischbeck KH, Burnett BG. Histone deacetylase inhibition suppresses myogenin-dependent atrogene activation in spinal muscular atrophy mice. *Hum Mol Genet* 2012;**21**:4448–4459.
15. Hellbach N, Peterson S, Haehnke D, Shankar A, LaBarge S, Pivaroff C, et al. Impaired myogenic development, differentiation and function in hESC-derived SMA myoblasts and myotubes. *PLoS ONE* 2018;**13**:e0205589.
16. Kong L, Wang X, Choe DW, Polley M, Burnett BG, Bosch-Marce M, et al. Impaired synaptic vesicle release and immaturity of neuromuscular junctions in spinal muscular atrophy mice. *J Neurosci* 2009;**29**:842–851.
17. Mutsaers CA, Wishart TM, Lamont DJ, Riessland M, Schreml J, Comley LH, et al. Reversible molecular pathology of skeletal muscle in spinal muscular atrophy. *Hum Mol Genet* 2011;**20**:4334–4344.
18. Ling KK, Gibbs RM, Feng Z, Ko CP. Severe neuromuscular denervation of clinically relevant muscles in a mouse model of spinal muscular atrophy. *Hum Mol Genet* 2012;**21**:185–195.
19. Shafey D, Cote PD, Kothary R. Hypomorphic Smn knockdown C2C12 myoblasts reveal intrinsic defects in myoblast fusion and myotube morphology. *Exp Cell Res* 2005;**311**:49–61.
20. Kim JK, Jha NN, Feng Z, Faleiro MR, Chiriboga CA, Wei-Lapierre L, et al. Muscle-specific SMN reduction reveals motor neuron-independent disease in spinal muscular atrophy models. *J Clin Invest* 2020;**130**:1271–1287.
21. Hua Y, Vickers TA, Okunola HL, Bennett CF, Krainer AR. Antisense masking of an hnRNP

A1/A2 intronic splicing silencer corrects SMN2 splicing in transgenic mice. *Am J Hum Genet* 2008;**82**:834–848.
22. Singh NK, Singh NN, Androphy EJ, Singh RN. Splicing of a critical exon of human survival motor neuron is regulated by a unique silencer element located in the last intron. *Mol Cell Biol* 2006;**26**:1333–1346.
23. Foust KD, Wang X, McGovern VL, Braun L, Bevan AK, Haidet AM, et al. Rescue of the spinal muscular atrophy phenotype in a mouse model by early postnatal delivery of SMN. *Nat Biotechnol* 2010;**28**:271–274.
24. Poirier A, Weetall M, Heinig K, Bucheli F, Schoenlein K, Alsenz J, et al. Risdiplam distributes and increases SMN protein in both the central nervous system and peripheral organs. *Pharmacol Res Perspect* 2018;**6**: e00447.
25. Finkel RS, Mercuri E, Darras BT, Connolly AM, Kuntz NL, Kirschner J, et al. Nusinersen versus sham control in infantile-onset spinal muscular atrophy. *N Engl J Med* 2017;**377**:1723–1732.
26. Mercuri E, Darras BT, Chiriboga CA, Day JW, Campbell C, Connolly AM, et al. Nusinersen versus sham control in later-onset spinal muscular atrophy. *N Engl J Med* 2018;**378**:625–635.
27. Darras BT, Chiriboga CA, Iannaccone ST, Swoboda KJ, Montes J, Mignon L, et al. Nusinersen in later-onset spinal muscular atrophy: long-term results from the phase 1/2 studies. *Neurology* 2019;**92**: e2492–e2506.
28. Mendell JR, Al-Zaidy S, Shell R, Arnold WD, Rodino-Klapac LR, Prior TW, et al. Single-dose gene-replacement therapy for spinal muscular atrophy. *N Engl J Med* 2017;**377**:1713–1722.
29. Kaifer KA, Villalon E, Osman EY, Glascock JJ, Arnold LL, Cornelison DDW, et al. Plastin-3 extends survival and reduces severity in mouse models of spinal muscular atrophy. *JCI Insight* 2017;**2**:e89970.
30. Millay DP, O'Rourke JR, Sutherland LB, Bezprozvannaya S, Shelton JM, Bassel-Duby R, et al. Myomaker is a membrane activator of myoblast fusion and muscle formation. *Nature* 2013;**499**:301–305.
31. Leikina E, Gamage DG, Prasad V, Goykhberg J, Crowe M, Diao J, et al. Myomaker and myomerger work independently to control distinct steps of membrane remodeling during myoblast fusion. *Dev Cell* 2018;**46**:767–780, e7.
32. Bi P, Ramirez-Martinez A, Li H, Cannavino J, McAnally JR, Shelton JM, et al. Control of muscle formation by the fusogenic micropeptide myomixer. *Science* 2017;**356**: 323–327.
33. Quinn ME, Goh Q, Kurosaka M, Gamage DG, Petrany MJ, Prasad V, et al. Myomerger induces fusion of non-fusogenic cells and is required for skeletal muscle development. *Nat Commun* 2017;**8**:15665.
34. Zhang Q, Vashisht AA, O'Rourke J, Corbel SY, Moran R, Romero A, et al. The microprotein minion controls cell fusion and muscle formation. *Nat Commun* 2017;**8**:15664.
35. Moritz KE, McCormack NM, Abera MB, Viollet C, Yauger YJ, Sukumar G, et al. The role of the immunoproteasome in interferon-gamma-mediated microglial activation. *Sci Rep* 2017;**7**:9365.
36. Abera MB, Xiao J, Nofziger J, Titus S, Southall N, Zheng W, et al. ML372 blocks SMN ubiquitination and improves spinal muscular atrophy pathology in mice. *JCI Insight* 2016;**1**:e88427.
37. Butchbach ME, Edwards JD, Burghes AH. Abnormal motor phenotype in the SMNDelta7 mouse model of spinal muscular atrophy. *Neurobiol Dis* 2007;**27**: 207–219.
38. Hindi SM, Tajrishi MM, Kumar A. Signaling mechanisms in mammalian myoblast fusion. *Sci Signal* 2013;**6**:re2.
39. Sampath SC, Sampath SC, Millay DP. Myoblast fusion confusion: the resolution begins. *Skelet Muscle* 2018;**8**:3.
40. Millay DP, Sutherland LB, Bassel-Duby R, Olson EN. Myomaker is essential for muscle regeneration. *Genes Dev* 2014;**28**: 1641–1646.
41. Luo W, Li E, Nie Q, Zhang X. Myomaker, regulated by MYOD, MYOG and miR-140-3p, promotes chicken myoblast fusion. *Int J Mol Sci* 2015;**16**:26186–26201.
42. Takei D, Nishi M, Fukada S, Doi M, Okamura H, Uezumi A, et al. Gm7325 is MyoD-dependently expressed in activated muscle satellite cells. *Biomed Res* 2017;**38**:215–219.
43. Bowerman M, Becker CG, Yanez-Munoz RJ, Ning K, Wood MJA, Gillingwater TH, et al. Therapeutic strategies for spinal muscular atrophy: SMN and beyond. *Dis Model Mech* 2017;**10**:943–954.
44. Martinez TL, Kong L, Wang X, Osborne MA, Crowder ME, Van Meerbeke JP, et al. Survival motor neuron protein in motor neurons determines synaptic integrity in spinal muscular atrophy. *J Neurosci* 2012;**32**:8703–8715.
45. Osman EY, Washington CW 3rd, Kaifer KA, Mazzasette C, Patitucci TN, Florea KM, et al. Optimization of morpholino antisense oligonucleotides targeting the intronic repressor element1 in spinal muscular atrophy. *Mol Ther* 2016;**24**: 1592–1601.
46. Walter MC, Wenninger S, Thiele S, Stauber J, Hiebeler M, Greckl E, et al. Safety and treatment effects of nusinersen in longstanding adult 5q-SMA type 3 - a prospective observational study. *J Neuromuscul Dis* 2019;**6**:453–465.
47. Rudnik-Schoneborn S, Lutzenrath S, Borkowska J, Karwanska A, Hausmanowa-Petrusewicz I, Zerres K. Analysis of creatine kinase activity in 504 patients with proximal spinal muscular atrophy types I-III from the point of view of progression and severity. *Eur Neurol* 1998;**39**:154–162.
48. Zalneraitis EL, Halperin JJ, Grunnet ML, Russman BS, Peress N. Muscle biopsy and the clinical course of infantile spinal muscular atrophy. *J Child Neurol* 1991;**6**: 324–328.
49. Lee YI, Mikesh M, Smith I, Rimer M, Thompson W. Muscles in a mouse model of spinal muscular atrophy show profound defects in neuromuscular development even in the absence of failure in neuromuscular transmission or loss of motor neurons. *Dev Biol* 2011;**356**: 432–444.
50. Hayhurst M, Wagner AK, Cerletti M, Wagers AJ, Rubin LL. A cell-autonomous defect in skeletal muscle satellite cells expressing low levels of survival of motor neuron protein. *Dev Biol* 2012;**368**: 323–334.
51. Faralli H, Dilworth FJ. Turning on myogenin in muscle: a paradigm for understanding mechanisms of tissue-specific gene expression. *Comp Funct Genomics* 2012;**2012**: 836374.
52. Petrany MJ, Song T, Sadayappan S, Millay DP. Myocyte-derived myomaker expression is required for regenerative fusion but exacerbates membrane instability in dystrophic myofibers. *JCI Insight* 2020;**5**:e136095.
53. De Vivo DC, Bertini E, Swoboda KJ, Hwu WL, Crawford TO, Finkel RS, et al. Nusinersen initiated in infants during the presymptomatic stage of spinal muscular atrophy: interim efficacy and safety results from the Phase 2 NURTURE study. *Neuromuscul Disord* 2019;**29**:842–856.
54. Deguise MO, Boyer JG, McFall ER, Yazdani A, De Repentigny Y, Kothary R. Differential induction of muscle atrophy pathways in two mouse models of spinal muscular atrophy. *Sci Rep* 2016; **6**:28846.
55. Rajendra TK, Gonsalvez GB, Walker MP, Shpargel KB, Salz HK, Matera AGC. A Drosophila melanogaster model of spinal muscular atrophy reveals a function for SMN in striated muscle. *J Cell Biol* 2007;**176**: 831–841.
56. Zhou H, Meng J, Malerba A, Catapano F, Sintusek P, Jarmin S, et al. Myostatin inhibition in combination with antisense oligonucleotide therapy improves outcomes in spinal muscular atrophy. *J Cachexia Sarcopenia Muscle* 2020;**11**:768–782.
57. Long KK, O'Shea KM, Khairallah RJ, Howell K, Paushkin S, Chen KS, et al. Specific inhibition of myostatin activation is beneficial in mouse models of SMA therapy. *Hum Mol Genet* 2019;**28**:1076–1089.
58. Hwee DT, Kennedy AR, Hartman JJ, Ryans J, Durham N, Malik FI, et al. The small-molecule fast skeletal troponin activator, CK-2127107, improves exercise tolerance in a rat model of heart failure. *J Pharmacol Exp Ther* 2015;**353**: 159–168.
59. von Haehling S, Morley JE, Coats AJS, Anker SD. Ethical guidelines for publishing in the *Journal of Cachexia, Sarcopenia and Muscle*: update 2019. *J Cachexia Sarcopenia Muscle* 2019;**10**:1143–1145.